C.P. No. 171
(15,177)
A.R.C. Technical Report

MINISTRY OF SUPPLY

AERONAUTICAL RESEARCH COUNCIL

CURRENT PAPERS

The Application of Camber and Twist to Swept Wings in Incompressible Flow

By

G. G. Brebner, M.A.

LONDON: HER MAJESTY'S STATIONERY OFFICE

1954

Price 5s. 6d. net

C.P.No.171

U.D.C. No. 533.691.11.011.3:533.691.11.043.2:
533.69.048.1/2:533.6.013.412

Report No. Aero 2458

March, 1952

ROYAL AIRCRAFT ESTABLISHMENT

The Application of Camber and Twist to Swept Wings in Incompressible Flow

by

G.G. Brebner, M.A.

SUMMARY

A certain type of chordwise vorticity distribution, applicable to a thin wing of any sweep in incompressible flow, is combined with the general equation for the downwash induced at any spanwise position on a swept wing by the spanwise vortices. By applying the "streamline condition" that there is no velocity component perpendicular to the wing surface, and integrating over the chord, the equation of a camber line is obtained. The initial vorticity distribution contains two parameters which are related to the amount of camber and the chordwise position of the maximum ordinate, and thus define a doubly infinite family of camber lines. Expressions are found for the effect of these camber lines on the zero lift angle, lift distribution and centre of pressure at all spanwise positions. Simple charts are provided from which may be read the equivalent incidence and pitching moment at zero lift of any camber line of the family at any spanwise position on a wing of any sweep.

A detailed description is given of the method of calculating the loading on a given cambered swept wing. Also, the design of wings incorporating camber and twist to produce required chordwise and spanwise loadings is treated in detail, and it is shown that at any spanwise position only one particular combination of camber and incidence will give a required chordwise loading. The correct matching of camber and twist over the whole wing is thus of fundamental importance. One particular camber line of the series, denoted by m = 0.5, is found to be exactly that required to eliminate the centre and tip effects on the chordwise loading of swept wings.

Brief mention is made of the effect of wing thickness on the lift distributions. The local lift coefficients are increased by about the same approximate factor as a symmetrical aerofoil section, namely $\left(1 + \frac{0.8 \times t/c}{\cos \varphi}\right)$. Formulae are given for the pressure distribution on a thick cambered aerofoil at any spanwise position.

LIST OF CONTENTS

LIST OF TABLES

LIST OF ILLUSTRATIONS

1 Introduction

In recent years symmetrical aerofoil sections have been more popular than cambered ones for use on wings of high-speed aircraft; while tests on unswept wings indicated that their high-speed aerodynamic characteristics at moderate C_L were at least as good as those of cambered sections, they were simpler to calculate and construct. During this period the use of sweepback to delay the drag rise with Mach number has become very common. The loading and pressure distribution on sweptback wings with a uniform aerofoil section everywhere are different from those on the corresponding unswept wings, and may require to be modified if the full benefit of sweepback is to be realised, or if some unwelcome penalties (e.g. unsatisfactory stalling characteristics) are to be avoided. If, as is usually the case, both the chordwise and spanwise loadings need modifying, this can only be done - if at all - by an appropriate combination of camber and twist, although initially the basic section may be uncambered. This is true not only throughout the subsonic speed range but also at supersonic speeds (e.g. Ref.1). Thus a simple method of calculating the loading of cambered swept wings, accurate enough for practical purposes, is required.

This report provides a method of calculating the effect of a certain type of camber on the chordwise and spanwise loadings of any wing, swept or unswept, in incompressible potential flow. The Prandtl-Glauert rule (or one of its refinements) may be used to apply the method to high subsonic Mach numbers. It is an extension of Ref.2, which dealt with the calculation of the lift distribution on thin wings of symmetrical section such that low aspect ratio effects could be neglected. The methods and assumptions used there form the basis of the present report. They are to be more fully explained in a later note and no detailed justifications will be given here.

As far as the spanwise loading is concerned, replacing a symmetrical aerofoil by a cambered one can always be interpreted as applying to the symmetrical section a certain twist or change of incidence, equal to the zero lift angle of the cambered section. But whereas uniform camber on an unswept wing imparts the same equivalent change of incidence (the zero lift angle of the two-dimensional section) at all spanwise positions, this is not so for a swept wing. Again, the chordwise loading of a thin symmetrical wing is usually assumed not to vary with the span if the wing is unswept (except for small aspect ratio), but it does so vary if the wing is swept. The effect of adding a uniform camber also varies along the span if the wing is swept. Thus the calculation of both the basic incidence term and the camber term in the chordwise loading is more complicated for a swept wing.

It is unlikely that an arbitrary camber line will lead to an equation for the circulation from which the usual quantities can be calculated, (e.g. lift, pitching moment, zero lift angle). It was therefore decided to start with a chordwise distribution of vorticity from which the aerodynamic characteristics could be deduced, and which would contain parameters determining the geometry of a family of camber lines. This vortex distribution, (which is placed on a straight line and not on the camber line, the usual assumptions of linearised theory being made,) is inserted in the characteristic downwash equation for swept wings,[2] and the resulting streamline through the leading or trailing edge determines the shape of a thin aerofoil. This shape is the camber line associated with the chordwise vortex distribution originally assumed: it contains the same parameters as the vortex distribution and thus a family of camber lines is obtained.

The family of camber lines used here gives chordwise loadings ranging, on a two-dimensional wing, from a constant value along the chord to a "flat-plate" type of distribution, thus covering the whole range of practical interest.

The calculation method described here applies to this family of camber lines. If the effect of camber on the spanwise loading only is required (i.e. the equivalent change of incidence) the method can probably be applied to any camber line of non-reflex shape. However the chordwise loadings and pitching moments apply only to camber lines of the present family and close approximations to them. With this proviso, the method may be applied to the calculation of the loadings of given finite cambered wings, the procedure of Ref. 2 being adapted for this purpose. Camber and twist may be used on swept wings to modify the chordwise and spanwise loadings so that they comply with requirements for high Mach numbers, high lift, etc. The method of this report may be used to design a wing with the appropriate amounts of camber and twist to achieve a desired loading.

In the text, the mean line between the upper and lower surfaces of a thick cambered aerofoil will be called the "camber line". The maximum ordinate of the camber line, referred to the local chord, will be called the "camber", and the chordwise position of the maximum ordinate will be called the "position of camber".

The following terms will be used to identify the various quantities associated with an aerofoil section on a wing. The term "two-dimensional" will refer to the aerofoil characteristics of an infinite unswept wing. "Sectional" $\left(\text{e.g. sectional lift slope, } \frac{\partial C_L}{\partial \alpha_e}\right)$ will refer to the aerofoil characteristics at any spanwise position arising only from the bound vortices* on the wing. Sectional characteristics include effects of planform (e.g. sweep, spanwise position), and camber, but not the effect of the trailing vortices. The term "local" $\left(\text{e.g. local lift slope, } \frac{\partial C_L}{\partial \alpha}\right)$ will refer to the aerofoil characteristics at any spanwise position arising from both the bound and trailing vortices. The effect of planform is again included. For example the local C_L at a spanwise position $y = y_1$ is that given by the spanwise loading curve at that position.

The report falls into two parts. The first part (section 2) contains the mathematical foundation of the calculation method, and may be omitted by any reader who is interested only in applying the results. The second part of the report consists of Sections 3, 4 and 5. In Section 3 the main results of Section 2 are summarised and discussed with a view to practical application. Section 4 describes in detail the calculation of the chordwise and spanwise loadings of a given wing, and the design of a wing incorporating camber and twist to have a required loading. In Section 5, the method of Ref.3 is adapted to calculate the pressure distribution over a thick cambered aerofoil.

Although the formulae may appear complicated at first sight, the practical application of the results is straightforward and easy, since tables and diagrams are provided from which most of the required information may be obtained, either directly or by interpolation. Tables I and II give the shapes of some members of the family of camber lines, all

---

* The conception of bound and trailing vortices on a swept wing will be discussed in a subsequent report.

calculated to give $C_L = 1.0$ on a two-dimensional wing at zero incidence. These camber lines and their chordwise loadings are shown in Figs.4 and 5. Figs 6 to 8 show the equivalent change of incidence and the pitching moment at zero lift plotted against a function given by the planform. They can be easily applied to any spanwise position on a swept wing.

2 Mathematical basis of the method

2.1 Derivation of the camber line equations

2.11 Preliminary remarks

The loading on a cambered aerofoil may be divided into two parts, one arising from the incidence of the aerofoil and the other from the camber. The camber effect may be expressed as an equivalent change of incidence $\Delta\alpha$, i.e. the incidence which would have to be added to the uncambered aerofoil to cause the same lift increment as the camber. On an unswept wing having uniform camber along the span, $\Delta\alpha$ is to all intents and purposes the same at all spanwise positions, and is of course the same at all incidences· the basic lift slope due to incidence, $\frac{\partial C_L}{\partial \alpha_e}$, is also the same at all spanwise positions. On a swept wing $\Delta\alpha$ at any spanwise position is still independent of incidence,[4] but both $\Delta\alpha$ and the basic incidence term are functions of the spanwise position.

Since sweep affects even the basic incidence term, consider first a thin wing of symmetrical section swept at an angle φ. For tapered wings we assume the angle of sweep to be that of the mid-chord line.* The restriction to thin wings means that only first order effects are considered. The chordwise distribution of vorticity at the centre of such a wing may be assumed to be of the form

$$\gamma_x(x) = 2V_0 \cos\varphi . \alpha_e \left(\frac{1-x}{x}\right)^{\frac{1}{2}} \left(1 - \frac{\varphi}{\pi/2}\right), \qquad (1)$$

where the x-axis is the chordline, x is made dimensionless with the local chord, and the vorticity is distributed along the chordline. α_e is the effective incidence, i.e. $\alpha_e = \alpha$ - total induced incidence from trailing vortices. The corresponding distribution for an infinite sheared wing is of the form

$$\gamma_x(x) = 2V_0 \alpha_e \left(\frac{1-x}{x}\right)^{\frac{1}{2}} \qquad (2)$$

At any intermediate section between the centre and mid-semispan (where the distribution is of the sheared wing type), the term containing x in the vortex distribution is of the form $\left(\frac{1-x}{x}\right)^n$ where n lies

---

* In the calculation method of Ref.2 the sweep angle is defined as that of the mid-chord line near the centre and tip and as that of the quarter-chord line near mid-semi-span. This is an unnecessary refinement when calculating the effect of camber. Throughout this report, φ means the sweep of the mid-chord line.

between $\frac{1}{2}$ and $\frac{1}{2}\left(1-\frac{\varphi}{\pi/2}\right)$: i.e.

$$n(\varphi, y) = \tfrac{1}{2}\left\{1-\lambda(y).\frac{\varphi}{\pi/2}\right\}, \qquad (3)$$

where y is the spanwise coordinate, dimensionless with the local chord. For an unswept wing, $\varphi = 0^{o}$ and $n(\varphi, y) = \frac{1}{2}$ at all spanwise position.

$\lambda(y)$ is a function of the spanwise coordinate y such that

$\lambda(y) = 1$ at the centre section

$\lambda(y) = 0$ at the "sheared part"

$0 < \lambda(y) < 1$ at intermediate positions.

Fig.1 (which is reproduced from Fig.1 of Ref.2) is a curve based on experimental data which shows how $\lambda(y)$ varies with y. $\lambda(y)$ may be obtained directly from Fig.1 for any spanwise station.

The general equation for the vortex distribution at any section between the centre and the sheared part of the wing may be written

$$\gamma_{x}(x) = 2V_{o} \sin \pi n.\alpha_{e}\left(\frac{1-x}{x}\right)^{n} \qquad (4)$$

where

$$n = \tfrac{1}{2}\left\{1-\lambda(y).\frac{\varphi}{\pi/2}\right\},$$

a known function of φ and y. This gives the assumed distributions at the centre and sheared part of the wing, viz.

$$n = \tfrac{1}{2}\left(1-\frac{\varphi}{\pi/2}\right): \quad \gamma_{x}(x) = 2V_{o} \cos \varphi.\alpha_{e}\left(\frac{1-x}{x}\right)^{\frac{1}{2}\left(1-\frac{\varphi}{\pi/2}\right)}$$

at the centre,

$$n = \tfrac{1}{2}: \quad \gamma_{x}(x) = 2V_{o}\,\alpha_{e}\left(\frac{1-x}{x}\right)^{\frac{1}{2}}$$

at the sheared part, and equation (4) is an interpolation formula for spanwise positions between these limits.

Equations (3) and (4) apply also to any section between the sheared part and the tip, $\lambda(y)$ then being negative.

$\lambda(y) = -1$ at the tip,

$\lambda(y) = 0$ at the sheared part,

$0 > \lambda(y) > -1$ at intermediate positions.

Fig.1 may still be used to find the magnitude of $\lambda(y)$, y in this case being measured inwards from the tip. Thus the vortex distributions at all spanwise stations of a swept wing of symmetrical aerofoil section may be found from equation (4).

2.12 The camber line equations

Consider now a thin cambered section at incidence. The vortex distribution may be resolved into a basic incidence term given by equation (4) and a term due only to camber at zero incidence. The latter is assumed to be of the type

$$\gamma_x(x) = 2V_o \sin \pi n . A_2 \left(\frac{1-x}{x}\right)^m, \qquad (5)$$

where A_2 and m are parameters depending on the shape of the camber line. This is no more than a conveniently chosen family of functions which will be developed to give a family of camber lines.

The incidence zero could reasonably be taken as the position at which the stagnation point is at the leading edge, or as the position of zero lift. However it is convenient to define it as the incidence at which the chordline Ox is parallel to the resultant wind direction V_o' (see Fig.2). This will not, in general, coincide with either of the other two definitions, and so it is to be expected that even at zero incidence there will be an "incidence term" in the expression for the chordwise vortex distribution.

The following type of chordwise vortex distribution along the x-axis is therefore taken for a thin cambered section on a swept wing:-

$$\gamma_x(x) = 2V_o \sin \pi n \left\{A_1 \left(\frac{1-x}{x}\right)^n + A_2 \left(\frac{1-x}{x}\right)^m\right\} \qquad (6)$$

The right-hand side may be resolved into

$$2V_o \sin \pi n . \alpha_e \left(\frac{1-x}{x}\right)^n ,$$

the basic incidence term, and

$$2V_o \sin \pi n \left\{(A_1 - \alpha_e) \left(\frac{1-x}{x}\right)^n + A_2 \left(\frac{1-x}{x}\right)^m\right\} ,$$

the term due to the camber at zero incidence.

For a wing of given planform, n is known for any spanwise position since it is a function of φ and y only. Equation (3) shows that $0 \leqslant n \leqslant \frac{1}{2}$ between the centre and the sheared part of sweptback wings (and between the sheared part and tip of sweptforward wings); $\frac{1}{2} \leqslant n \leqslant 1$ between

the sheared part and tip of sweptback wings (and between the centre and sheared part of sweptforward wings). n is essentially a parameter associated with the basic incidence term. A_1, A_2 and m on the other hand, are those constants, as yet unknown, which are essentially connected with the shape of the camber line. However m may already be restricted to the range $0 \leqslant m \leqslant 1$: $0 \leqslant m$ is necessary in order to have zero vorticity at the trailing edge with the flow leaving the trailing edge tangentially (Joukowski's hypothesis); $m < 1$ is necessary to avoid an infinite value of local lift coefficient when $\gamma_x(x)$ is integrated over the chord; $m = 1$ appears to give such an infinite lift coefficient, but it will be seen that A_2 then becomes zero and $m = 1$ is a permissible value of the exponent.

Equation (4) fulfils the requirement mentioned in Section 1 that the vortex distribution may be manipulated to give aerodynamic properties such as lift, pitching moment and zero lift angle.

Fig.2 shows the axes used. The x-axis lies along the chordline which, following NACA convention, joins the ends of the camber line, and makes an angle α with the true wind direction. With the sign convention of Fig.2 the following expression for the downwash due to the bound vortices at any spanwise position on a swept wing is used* (see equation (7) in Appendix I of Ref.2):-

$$\frac{v_z}{V_o} = \frac{1}{2\pi V_o} \left\{ \int_o^1 \gamma_x(x') \frac{dx'}{(x - x')} + \frac{\pi}{\tan \pi n} \gamma_x(x) \right\} \qquad (7)$$

Now

$$\int_o^1 \left(\frac{1 - x'}{x'} \right)^p \cdot \frac{dx'}{x - x'} = K_1(p) - K_2(p) \left(\frac{1 - x}{x} \right)^p \qquad (8)$$

for $0 \leqslant p \leqslant 1$

where

$$K_1(p) = \frac{1}{p} \int_o^\infty \frac{ds}{1 + s^{1/p}} = \frac{\pi}{\sin \pi p} \qquad (9)$$

and

$$K_2(p) = \frac{1}{p} \int_o^\infty \frac{ds}{1 - s^{1/p}} = \frac{\pi}{\tan \pi p} \qquad (10)$$

---

* This equation, which forms the basis of the present method has been derived in Ref.2 for the centre and sheared part of a swept wing, and will be further discussed in a later note. It has been checked by an experiment designed for that purpose. A certain distribution of $\gamma_x(x)$ was chosen for the centre of a swept wing, and v_z/V_o, evaluated from equation (7), was used to define the mean line at the centre. Pressure measurements showed that the chosen $\gamma_x(x)$ had been obtained (Ref.4). Here, equation (7) is also used to interpolate between centre and sheared part.

Therefore, from (6) and (7),

$$\frac{v_z}{V_o} = \frac{\sin \pi n}{\pi} \left\{ A_1 \left[K_1(n) - \left(K_2(n) - \frac{\pi}{\tan \pi n} \right) \left(\frac{1-x}{x} \right)^n \right] + A_2 \left[K_1(m) - \left(K_2(m) - \frac{\pi}{\tan \pi n} \right) \left(\frac{1-x}{x} \right)^m \right] \right\} \qquad (11)$$

$$= \frac{\sin \pi n}{\pi} \left\{ A_1 \frac{\pi}{\sin \pi n} + A_2 \left[\frac{\pi}{\sin \pi m} - \left(\frac{\pi}{\tan \pi m} - \frac{\pi}{\tan \pi n} \right) \left(\frac{1-x}{x} \right)^m \right] \right\} \qquad (12)$$

from equations (9) and (10)

$$= A_1 + A_2 \left[\frac{\sin \pi n}{\sin \pi m} - \sin \pi n \left(\cot \pi m - \cot \pi n \right) \left(\frac{1-x}{x} \right)^m \right] \qquad (13)$$

From the streamline condition, $\frac{V_z}{V_x} = \frac{dz}{dx}$, for the flow past a thin cambered aerofoil,

$$\frac{v_z + v_{zi} - V_o \sin \alpha}{V_o \cos \alpha} = \frac{dz}{dx} , \qquad (14)$$

where v_{zi} is the downwash induced by the trailing vortices and z is made non-dimensional with the local chord. If α is not large,

$$\cos \alpha \doteq 1$$

$$\sin \alpha \doteq \alpha .$$

Also, $\frac{v_{zi}}{V_o} = \alpha_i$, assumed to be constant over the chord (see Ref.2).

Therefore,

$$\frac{v_z}{V_o} + \alpha_i - \alpha = \frac{dz}{dx} ,$$

i.e.,

$$\frac{v_z}{V_o} = \alpha_e + \frac{dz}{dx} \qquad (15)$$

Combining equations (13) and (15),

$$\alpha_e + \frac{dz}{dx} = A_1 + A_2 \frac{\sin \pi n}{\sin \pi m} - A_2 \sin \pi n \left(\cot \pi m - \cot \pi n \right) \left(\frac{1-x}{x} \right)^m \qquad (16)$$

Integrating with respect to x, and noting that $z = 0$ when $x = 0$,

$$z = \left(-\alpha_e + A_1 + A_2 \frac{\sin \pi n}{\sin \pi m}\right) x - A_2 \sin \pi n \, (\cot \pi m - \cot \pi n) \int_0^x \left(\frac{1 - x'}{x'}\right)^m dx' \tag{17}$$

$\int_0^x \left(\frac{1 - x'}{x'}\right)^m dx'$ is a function of x and m for which we have no explicit expression in general.

Putting $\quad s' = \left(\frac{1 - x'}{x'}\right)^m , \quad s = \left(\frac{1 - x}{x}\right)^m ,$

$$\int_0^x \left(\frac{1 - x'}{x'}\right)^m dx' = \int_s^\infty \frac{ds'}{1 + s'^{1/m}} + x \left(\frac{1 - x}{x}\right)^m$$

It may be noted that, when $x = 1$,

$$\int_0^1 \left(\frac{1 - x'}{x'}\right)^m dx' = \int_0^\infty \frac{ds'}{1 + s'^{1/m}} = m.K_1(m) = \frac{\pi m}{\sin \pi m} \tag{18}$$

$\int_s^\infty \frac{ds'}{1 + s'^{1/m}}$ has been evaluated graphically in the calculations for this report, and is denoted by $B(x,m)$: i.e.

$$B(x,m) = \int_s^\infty \frac{ds'}{1 + s'^{1/m}} , \tag{19}$$

where s' and s are as defined above.

Equation (17) now becomes

$$z = \left(-\alpha_e + A_1 + A_2 \frac{\sin \pi n}{\sin \pi m}\right) x - A_2 \sin \pi n \, (\cot \pi m - \cot \pi n) \left[B(x,m) + x \left(\frac{1 - x}{x}\right)^m\right]$$

From Fig.2, $z = 0$ at $x = 1$.

i.e. $$0 = \left(-\alpha_e + A_1 + A_2 \frac{\sin \pi n}{\sin \pi m}\right) - A_2 \sin \pi n \, (\cot \pi m - \cot \pi n) \frac{\pi m}{\sin \pi m}$$

$$\text{i e} \quad \alpha_e = A_1 + A_2 \frac{\sin \pi n}{\sin \pi m} \{1 - \pi m \, (\cot \pi m - \cot \pi n)\} \tag{20}$$

Equation (20) enables A_1 to be eliminated from equation (6), and leads to -

$$z = A_2 \sin \pi n \, (\cot \pi m - \cot \pi n) \left[\frac{\pi m}{\sin \pi m} x - B(x,m) - x \left(\frac{1-x}{x} \right)^m \right] \tag{21}$$

This is the equation of the family of camber lines, the parameters being n (associated with the planform and basic incidence term), and A_2 and m (associated with the camber) The next step is to determine m and A_2 in terms of the geometry of the camber lines

2 13 Relation of A_2 and m to the camber and position of camber

From equations (16), (20) and (21),

$$\frac{dz}{dx} = \frac{\frac{\pi m}{\sin \pi m} - \left(\frac{1-x}{x} \right)^m}{\frac{\pi m}{\sin \pi m} x - B(x,m) - x \left(\frac{1-x}{x} \right)^m} \, z \tag{22}$$

For certain values of m and n it is not possible to evaluate z and $\frac{dz}{dx}$ from equations (21) and (22) in a straightforward manner For instance when $m = 0$, $\cot \pi m = \infty$ and when $m = n$, $\cot \pi m - \cot \pi n = 0$ Such special cases are dealt with in Section 2 3

$\frac{dz}{dx}$ is the slope of the camber line, and at the position of camber where z is a maximum $\frac{dz}{dx} = 0$ Therefore, by equation (22),

$$\frac{\pi m}{\sin \pi m} = \left(\frac{1-x}{x} \right)^m ,$$

ignoring trivial solutions of $\frac{dz}{dx} = 0$

$$\text{i e} \qquad x_f = \frac{1}{1 + \left(\frac{\pi m}{\sin \pi m} \right)^{1/m}} \tag{23}$$

where x_f is the coordinate of the position of camber Thus m determines, or is determined by, x_f, depending on which is given initially

From equation (21),

$$z_{max} = -A_2 \sin \pi n \, (\cot \pi m - \cot \pi n) \, B(x_f, m) \tag{24}$$

where z_{max} is the camber and

$$B(x_f,m) = \int_{\frac{\pi m}{\sin \pi m}}^{\infty} \frac{ds'}{1+s'^{1/m}} \qquad (25)$$

$$\left[s_f = \left(\frac{1-x_f}{x_f}\right)^m = \frac{\pi m}{\sin \pi m} \right]$$

$B(x_f,m)$ is a function of m only, since x_f is a function of m only. $B(x_f,m) \to \infty$ as $m \to 1$. To obtain a function which is finite everywhere in the range $0 \leqslant m \leqslant 1$, write

$$C(m) = \frac{1}{4.53} \cdot \frac{\pi m}{B(x_f,m)}$$

$$\text{i.e.} \qquad B(x_f,m) = \frac{1}{4.53} \cdot \frac{\pi m}{C(m)}$$

$B(x_f,m)$ was obtained by graphical integration. $C(m)$ varies between 0 and 1, and is plotted against m in Fig.3, along with x_f.

It should be noted that, using the coordinate system of Fig.2, a positive camber line in the usual sense corresponds to negative values of z. This accounts for the minus sign in equation (24), which may be rewritten:-

$$f = \frac{A_2 \sin \pi n \,.\, (\cot \pi m - \cot \pi n) \,.\, \pi m}{4.53\ C(m)} \qquad (26)$$

where $f = -z_{max}$.

$$\text{i.e.} \qquad A_2 = \frac{4.53\ C(m) \,.\, f}{\sin \pi n\ (\cot \pi m - \cot \pi n) \,.\, \pi m} \qquad (27)$$

Thus it is now possible to write the vortex distribution of equation (6) as a function of n, α_e, m and f:-

$$\gamma_x(x) = 2V_o \sin \pi n \left\{ \alpha_e \left(\frac{1-x}{x}\right)^n + \frac{4.53\ C(m) \,.\, f}{\sin \pi n} \left(\frac{1-x}{x}\right)^m \times \right.$$

$$\left. \left[\frac{1}{\pi m\ (\cot \pi m - \cot \pi n)} - \frac{\sin \pi n}{\sin \pi m} \left(\frac{1}{\pi m\ (\cot \pi m - \cot \pi n)} - 1 \right) \left(\frac{1-x}{x}\right)^{(n-m)} \right] \right\} \qquad (28)$$

where m and n are given by equations (23) and (3) respectively.

Equations (21 and (22) become

$$z = \frac{4.53\ C(m)\ .\ f}{\pi\, m}\left\{\frac{\pi m}{\sin \pi m}\, x - B(x,m) - x\left(\frac{1-x}{x}\right)^m\right\} \qquad (29)$$

$$\frac{dz}{dx} = \frac{4.53\ C(m)\ .\ f}{\pi\, m}\left\{\frac{\pi m}{\sin \pi m} - \left(\frac{1-x}{x}\right)^m\right\} \qquad (30)$$

Fig.4 shows some camber lines designed to give a $C_L = 1.0$ on a two-dimensional wing at zero incidence, and Fig.5 shows their chordwise loadings.

2.2 Aerodynamic properties

The aerodynamic properties of the family of thin cambered aerofoils given by equation (29) may be deduced from the vortex distribution of equation (28).

2.21 Chordwise loading

The streamlines over a swept wing are, in general, curved, and not straight lines in the free stream direction as for an unswept wing of infinite aspect ratio. This is because the velocity increments due to the vortex distribution are in the direction perpendicular to the vortex filaments $\gamma_x(x).dx$. If V_o is resolved into two components, one perpendicular and the other parallel to the vortex filament at that point, the velocity increments are added only to the former component. The latter is unchanged along a streamline. If the tangent to the vortex filament at any point has a sweep angle φ_V, then the two components of the free stream velocity are $V_o \cos \varphi_V$ and $V_o \sin \varphi_V$. Increments are added to $V_o \cos \varphi_V$ to give the velocities perpendicular to the filaments on the upper and lower surfaces.

φ_V is a function of y. At the centre section the streamline is in the free stream direction and $\cos \varphi_V = 1$: at the sheared part the filaments have a sweep angle equal to φ and therefore $\cos \varphi_V = \cos \varphi$. i.e.:-

$\cos \varphi_V = \cos \varphi$ at the sheared part and 1 at the centre. From Section 2.1,

$\sin \pi n = 1$ at the sheared part and $\cos \varphi$ at the centre.

Hence $\sin \pi n \times \cos \varphi_V = \cos \varphi$ at the centre and at the sheared part. This suggests that the formula may be a convenient interpolation for other spanwise positions:

$$\text{i.e.} \qquad \cos \varphi_V = \frac{\cos \varphi}{\sin \pi n}$$

The vortex system consists not of straight lines with a kink, but lines curved to achieve a continuous tangent over the whole span.

In general, φ_V varies along the chord at any spanwise position. The above relation is therefore only an approximation for a mean value of φ_V.

If the X and Y axes are perpendicular and parallel respectively to the vortex filament at any point, the velocity increments perpendicular to the filament on the upper and lower surfaces are $\pm \gamma_X(X)/2$, the vorticity distribution per unit area along the X-axis. The vorticity on an elementary area surrounding the point must be the same when referred to both sets of axes: i.e. $\gamma_x(x),dx,dy = \gamma_X(X).dX.dY$. From the usual transformation for rotation of axes, the area dx.dy = the area dX.dY.

Therefore $\gamma_x(x) = \gamma_X(X)$ and the velocity increments perpendicular to the vortex filament are $\pm \gamma_x(x)/2$.

The velocity components perpendicular to the vortex filaments on the upper and lower surfaces are therefore

$$(V_{perp})_{U.S.} = V_o \frac{\cos\varphi}{\sin\pi n} + \frac{\gamma_x(x)}{2}$$

$$(V_{perp})_{L.S.} = V_o \frac{\cos\varphi}{\sin\pi n} - \frac{\gamma_x(x)}{2}$$

The velocity component parallel to the filaments is

$$(V_{par}) = V_o \sin\varphi_V = V_o \sqrt{1 - \frac{\cos^2\varphi}{\sin^2\pi n}}$$

on both upper and lower surfaces.

Therefore $$(C_p)_{U.S.}(x) = 1 - \left(\frac{V_{U.S.}}{V_o}\right)^2$$

$$= 1 - \frac{\left(V_o \frac{\cos\varphi}{\sin\pi n} + \frac{\gamma_x(x)}{2}\right)^2 + V_o^2\left(1 - \frac{\cos^2\varphi}{\sin^2\pi n}\right)}{V_o^2}$$

$$= -\frac{\gamma_x(x)}{V_o} \cdot \frac{\cos\varphi}{\sin\pi n} - \left(\frac{\gamma_x(x)}{2V_o}\right)^2 .$$

and $$(C_p)_{L.S.}(x) = +\frac{\gamma_x(x)}{V_o} \cdot \frac{\cos\varphi}{\sin\pi n} - \left(\frac{\gamma_x(x)}{2V_o}\right)^2$$

Therefore $$\Delta C_p(x) = (C_p)_{U.S.}(x) - (C_p)_{L.S.}(x)$$

$$= -2 \cdot \frac{\gamma_x(x)}{V_o} \cdot \frac{\cos\varphi}{\sin\pi n} \qquad (31)$$

From (28) and (31),

$$\Delta C_p(x) = -4 \cos\varphi \left\{ \alpha_e \left(\frac{1-x}{x}\right)^n + \frac{4.53\, C(m)\,.\,f}{\sin \pi n} \left(\frac{1-x}{x}\right)^m \times \right.$$

$$\left. \left[\frac{1}{\pi m(\cot \pi m - \cot \pi n)} - \frac{\sin \pi n}{\sin \pi m} \left(\frac{1}{\pi m(\cot \pi m - \cot \pi n)} - 1 \right) \left(\frac{1-x}{x}\right)^{(n-m)} \right] \right\} \qquad (32)$$

2.22 Lift coefficient

The foregoing results are now used to determine some of the sectional aerodynamic characteristics at any spanwise position on a cambered swept wing.

$$C_L = -\int_0^1 \Delta C_p(x).dx$$

$$= 4 \cos\varphi \left\{ A_1 \int_0^1 \left(\frac{1-x}{x}\right)^n dx + A_2 \int_0^1 \left(\frac{1-x}{x}\right)^m dx \right\}$$

from equations (6) and (31)

$$= 4 \cos\varphi \left\{ A_1 \frac{\pi n}{\sin \pi n} + A_2 \frac{\pi m}{\sin \pi m} \right\} \qquad (33)$$

$$= 4 \frac{\cos\varphi}{\sin \pi n} \left\{ \alpha_e . \pi n + \frac{4.53\, C(m).f}{\sin \pi m\, (\cot \pi m - \cot \pi n)} \times \right.$$

$$\left. \left[\pi n\, (\cot \pi m - \cot \pi n) + 1 - \frac{n}{m} \right] \right\} \qquad (34)$$

The C_L due to a thin symmetrical section is obtained by putting $f = 0$ in (34). Then

$$C_{L_{\substack{\text{incidence} \\ \text{only}}}} = 4 \frac{\cos\varphi}{\sin \pi n} . \alpha_e . \pi n \qquad (35)$$

which gives the well-known expressions

$C_L = 2\pi\alpha_e$, on a two-dimensional wing (i.e. $\varphi = 0^\circ$, $n = \frac{1}{2}$)

$C_L = 2\pi\alpha_e \cos\varphi$, on a sheared wing (i.e. $\varphi \neq 0^\circ$, $n = \frac{1}{2}$)

$C_L = 2\pi\alpha_e \left(1 - \frac{\varphi}{\pi/2}\right)$, at the centre section of a sweptback wing

$\left(\text{i.e. } \varphi \neq 0^\circ,\ n = \frac{1}{2}\left(1 - \frac{\varphi}{\pi/2}\right)\right)$.

Therefore the additional lift due to camber may be written:-

$$\frac{\Delta C_L}{f} = 4 \frac{\cos \varphi}{\sin \pi n} \cdot \frac{4.53\ C(m)}{\sin \pi m\ (\cot \pi m - \cot \pi n)} \left[\pi n\ (\cot \pi m - \cot \pi n) + 1 - \frac{n}{m} \right] \quad (36)$$

2.23 Angle of zero lift

$\Delta\alpha$ is the amount by which the incidence of a thin symmetrical section would have to be increased to give the same lift increment as the camber. Therefore the angle of zero lift of the cambered section is $-\Delta\alpha$.

$\Delta\alpha$ is obtained from equation (36) by the relation

$$\Delta C_L = \frac{\partial C_L}{\partial \alpha_e} \cdot \Delta\alpha$$

From equation (34),

$$\frac{\partial C_L}{\partial \alpha_e} = 4\pi n \frac{\cos \varphi}{\sin \pi n} \quad (37)$$

Therefore

$$\frac{\Delta\alpha}{f} = \frac{\Delta C_L}{f} \cdot \frac{1}{\partial C_L / \partial \alpha_e}$$

$$= \frac{4.53\ C(m)}{\pi n \sin \pi m\ (\cot \pi m - \cot \pi n)} \left[\pi n\ (\cot \pi m - \cot \pi n) + 1 - \frac{n}{m} \right] \quad (38)$$

2.24 Pitching moment and centre of pressure

The pitching moment about the quarter-chord point is given by:-

$$C_m = - \int_0^1 \Delta C_p(x) . (\tfrac{1}{4} - x) . dx$$

$$= \frac{2}{V_o} \cdot \frac{\cos \varphi}{\sin \pi n} \int_0^1 \gamma_x(x) (\tfrac{1}{4} - x) . dx$$

$$= 4 \cos \varphi \left\{ \tfrac{1}{4} A_1 \frac{\pi n}{\sin \pi n} (2n-1) + \tfrac{1}{4} A_2 \frac{\pi m}{\sin \pi m} (2m-1) \right\} \quad (39)$$

$$= \cos \varphi \left\{ \alpha_e \frac{\pi n}{\sin \pi n} (2n-1) + A_2 \frac{\pi m}{\sin \pi m} \left[(2m-1) + (2n-1) \left\{ \pi n (\cot \pi m - \cot \pi n) - \frac{n}{m} \right\} \right] \right\} \quad (40)$$

When there is no camber, $A_2 = 0$ and then

$$\left[C_m\right]_\alpha = (2n-1)\cos\varphi.\,\alpha_e \frac{\pi n}{\sin \pi n}$$

Therefore the change in pitching moment due to camber is given by

$$\frac{\Delta C_m}{f} = \frac{4.53\ C(m).\cos\varphi}{\sin\pi(n-m)}\left[(2m-1)+(2n-1)\left\{\pi n\ (\cot \pi m - \cot \pi n) - \frac{n}{m}\right\}\right] \quad (41)$$

The local centre of pressure due to both incidence and camber effects may be found from equations (33) and (39) which give

$$C_m = \frac{2n-1}{4} C_L - \frac{9.06.C(m).f.\cos\varphi.(m-n)}{\sin\pi(m-n)} \quad (42)$$

$$= \frac{2n-1}{4} C_L + C_{m_o},$$

where C_{m_o} is the pitching moment coefficient at zero lift.

Therefore
$$\Delta x_{C.P.} = -\frac{C_m}{C_L} = -\frac{2n-1}{4} - \frac{C_{m_o}}{C_L} = \frac{\lambda\varphi}{2\pi} - \frac{C_{m_o}}{C_L} \quad (43)$$

The sectional centre of pressure due to the camber effect only may be found from equations (36) and (41):-

$$\left[\Delta x_{C.P.}\right]_f = -\frac{\Delta C_m}{\Delta C_L} = -\frac{2n-1}{4} - \frac{m-n}{2\left\{\pi n\ (\cot \pi m - \cot \pi n) + 1 - \frac{n}{m}\right\}} \quad (44)$$

$$= \frac{\lambda\varphi}{2\pi} - \frac{m-n}{2\left\{\pi n\ (\cot \pi m - \cot \pi n) + 1 - \frac{n}{m}\right\}}$$

The effect of the trailing vortices arising from the camber lift distribution will be included in the incidence lift distribution for which the C.P. position is given by

$$\left[\Delta x_{C.P}\right]_\alpha = \frac{\lambda\varphi}{2\pi} \qquad \text{[cf. Ref.2, Appendix I.]} \quad (45)$$

Equations (44) and (45) may be combined to give the same result as (42) if the separate lift coefficients due to camber and incidence are known.

2.3 Special values of m

There are several values of m which are of special interest, or at which the formulae of Sections 2.1 and 2.2 may require special treatment. These will be dealt with in this paragraph.

2.31 The case m = 0

This is the case of camber at $x_f = 0.50$ (see equation (23)). On a two-dimensional wing the distribution of $\gamma_x(x)$ and $\Delta C_p(x)$ associated with this camber line for $\alpha_e = 0$ is constant along the chord (Fig.5). It is a convenient camber line for practical application, as will be shown in Section 4. Putting $m = 0$ in the equations of Sections 2.1 and 2.2 introduces infinities and zeros. It is best to derive the equations afresh.

Equations (6) and (11) become respectively,

$$\gamma_x(x) = 2V_o \sin \pi n \left\{ A_1 \left(\frac{1-x}{x} \right)^n + A_2 \right\}$$

$$\frac{v_z}{V_o} = \frac{\sin \pi n}{\pi} \left\{ \int_o^1 A_1 \left(\frac{1-x'}{x'} \right)^n \frac{dx'}{x-x'} + \int_o^1 A_2 \frac{dx'}{x-x'} + A_2 \cdot \frac{\pi}{\tan \pi n} \right\}$$

$$= A_1 + A_2 \frac{\sin \pi n}{\pi} \int_o^1 \frac{dx'}{x-x'} + A_2 \cos \pi n$$

$$= A_1 - A_2 \frac{\sin \pi n}{\pi} \log \left(\frac{1-x}{x} \right) + A_2 \cos \pi n$$

$$= \frac{dz}{dx} + \alpha_e$$

Following the procedure of Section 2.1 the corresponding equation to (21) is

$$z = A_2 \frac{\sin \pi n}{\pi} \{x \log x + (1-x) \log (1-x)\} \qquad (46)$$

Also $A_1 = \alpha_e - A_2 \cos \pi n$, and $A_2 = \frac{4.53\, f}{\sin \pi n}$ (putting $x = 0.5$ in (46))

Therefore

$$z = \frac{4.53\, f}{\pi} \{x \log x + (1-x) \log (1-x)\} \qquad (47)$$

and $$\gamma_x(x) = 2V_o \sin \pi n \left\{ \alpha_e \left(\frac{1-x}{x}\right)^n + \frac{4.53\, f}{\sin \pi n} \left[1 - \cos \pi n \left(\frac{1-x}{x}\right)^n \right] \right\} \qquad (48)$$

The aerodynamic characteristics follow as in Section 2.2 and are:-

$$\frac{\Delta C_L}{f} = 18.12 \frac{\cos \varphi}{\sin \pi n} (1 - \pi n \cot \pi n) \qquad (49)$$

$$\frac{\Delta \alpha}{f} = \frac{4.53}{\pi n} (1 - \pi n \cot \pi n) \qquad (50)$$

$$\frac{\Delta C_m}{f} = - 4.53 \frac{\cos \varphi}{\sin \pi n} [1 + (2n - 1)\, \pi n . \cot \pi n] \qquad (51)$$

2.32 The case m = 1

This case is the opposite extreme to m = 0. It will be shown that it represents a straight line (i.e. a flat plate) at incidence. Again direct substitution in the equations of Sections 2.1 and 2.2 does not give the shape of the camber line and the aerodynamic properties, so a fresh start is made.

Equation (6) becomes

$$\gamma_x(x) = 2V_o \sin \pi n \left\{ A_1 \left(\frac{1-x}{x}\right)^n + A_2 \left(\frac{1-x}{x}\right) \right\}$$

$$C_L = - \int_o^1 \Delta C_p(x).dx = \frac{2}{V_o} \cdot \frac{\cos \varphi}{\sin \pi n} \int_o^1 \gamma_x(x) dx$$

$$= 4 \cos \varphi \left\{ A_1 \int_o^1 \left(\frac{1-x}{x}\right)^n dx + A_2 \int_o^1 \left(\frac{1-x}{x}\right) dx \right\}.$$

But $$\int_o^X \left(\frac{1-x}{x}\right) dx \to \infty \quad \text{as} \quad X \to 1.$$

Therefore, if the sectional C_L is to be finite, $A_2 = 0$, and

$$\gamma_x(x) = 2V_o \sin \pi n . A_1 \left(\frac{1-x}{x}\right)^n$$

This is the distribution for a "flat-plate" section on a swept wing, and it gives a "camber line"

$$z = (A_1 - \alpha_e)x + \text{const.}$$

Previously, $z = 0$ at $x = 1$. i.e. $z = (A_1 - \alpha_e)(x - 1)$,

and $z = 0$ at $x = 0$:

i.e. $A_1 = \alpha_e$ and $z = 0$ for all x. Thus the camber line has degenerated into a straight line, the vortex distribution being

$$\gamma_x(x) = 2V_0 \sin \pi n . \alpha_e \left(\frac{1-x}{x}\right)^n$$

However, by considering a family of camber lines having the same C_L it is seen that the limit as $m \to 1$ is a flat plate at an incidence $(\alpha_e + \alpha_f)$, the lift which was formerly due to camber being now obtained from the additional incidence α_f, (Fig.4). Equation (23) shows that $x_f = 0$ and therefore $z = -f$ at $x = 0$, instead of $z = 0$ as used above to eliminate A_1.

The equation of the camber line defined by $m = 1$ is therefore

$$z = (x - 1).f, \qquad (52)$$

a flat plate at incidence $\alpha_f = f$ radians. Therefore

$$\gamma_x(x) = 2V_0 \sin \pi n \, (\alpha_e + f) \left(\frac{1-x}{x}\right)^n \qquad (53)$$

When $m = 1$, $\frac{\Delta\alpha^0}{f} = 57.3$ for all values of φ, $\Delta\alpha$ being in degrees and f as before being dimensionless with the chord. The equations for the lift and pitching moment coefficients follow as before:-

$$\frac{\Delta C_L}{f} = 4 \cos \varphi . \frac{\pi n}{\sin \pi n} \qquad (54)$$

$$\frac{\Delta C_m}{f} = (2n - 1) \cos\varphi \frac{\pi n}{\sin \pi n} \qquad (55)$$

2.33 The case $m = n$

Since $0 \leqslant m \leqslant 1$ and $0 \leqslant n \leqslant 1$, it is possible for a certain combination of camber, sweep and spanwise position to make $m = n$. When this happens, the equations of Sections 2.1 and 2.2 may become indeterminate and will have to be solved by l' Hôpital's rule, viz:-

If $f(x) = g(x) = 0$ when $x = x_1$, then

$$\left[\frac{f(x)}{g(x)}\right]_{x = x_1} = \left[\frac{f'(x)}{g'(x)}\right]_{x = x_1} ,$$

provided $f'(x)$ and $g'(x)$ are not both zero at $x = x_1$. For instance when $m = n = 0.5$, $\frac{\Delta\alpha}{f}$ becomes indeterminate. Applying the above rule to equation (38) gives

$$\left(\frac{\Delta\alpha}{f}\right)_{m=n} = \left[\frac{\frac{d}{dm}\ (\text{numerator})}{\frac{d}{dm}\ (\text{denominator})}\right]_{m=n} + \frac{4.53\ C(m)}{\sin \pi m}$$

$$= -\frac{\sin \pi m}{\pi m \,.\, B(x_f, m)} + \frac{4.53\ C(m)}{\sin \pi m}$$

$$= \frac{4.53\ C(m)}{\sin \pi m}\left\{1 - \left(\frac{\sin \pi m}{\pi m}\right)^2\right\}$$

For example, let $m = n = 0.5$. Then

$$\frac{4.53\ C(m)}{\sin \pi m} = 4.53 \times 0.614, \quad \text{and} \quad \left(\frac{\sin \pi m}{\pi m}\right)^2 = 0.405.$$

Therefore $\frac{\Delta\alpha^o}{f} = 95$.

This process may be used to evaluate other functions of m and n which become indeterminate. For example, the vortex distribution becomes

$$\gamma_x(x) = 2V_o \sin \pi m \left(\frac{1-x}{x}\right)^m \times \left\{\alpha_e - \frac{4.53\ C(m)\,.\,f\,.\,\sin \pi m}{\pi^2 m}\left[\pi \cot \pi m - \frac{\pi^2 m}{\sin^2 \pi m} + \log\left(\frac{1-x}{x}\right)\right]\right\} \quad (56)$$

By ordinary substitution A_2 appears to become infinite.

3 Interpretation of the formulae

3.1 The family of camber lines

In Section 2, equation (29) defines a family of camber lines characterised by two parameters only. These parameters are:-

(i) the camber, f;

(ii) the position of camber, x_f.

Any member of this family has a chordwise vortex distribution of the type given by equation (6) in which the index m is a function of x_f only. This functional relationship is stated in equation (23):-

$$x_f = \frac{1}{1 + \left(\frac{\pi m}{\sin \pi m}\right)^{\frac{1}{m}}} , \qquad (23)$$

and illustrated in Fig.3. In the equations of the camber lines and their aerodynamic properties, m is used as the parameter of the position of camber instead of the more cumbersome x_f. $0 \leqslant m \leqslant 1$ means that $0.5 \geqslant x_f \geqslant 0$. The calculation method is not applicable to negative values of m (i.e. $0.5 \leqslant x_f \leqslant 1$) since the Joukowski condition that the flow leaves the trailing edge smoothly would not be complied with.

Equation (29) gives the shapes of the family of camber lines:-

$$z = \frac{4.53\ C(m).f}{\pi m} \left\{ \frac{\pi m}{\sin \pi m} x - B(x,m) - x\left(\frac{1-x}{x}\right)^m \right\} \qquad (29)$$

It will be seen that the chordwise variation of z depends only on $m(x_f)$. Fig.4 shows a number of camber lines derived from equation (29) by inserting different values of m. The camber, f, in each case is chosen to give a lift coefficient $\Delta C_L = 1.0$ at zero incidence on a two-dimensional wing. The extreme case of $m = 1$ represents a flat plate at an incidence of f radians. The other extreme, $m = 0$, gives a constant-load camber line. The co-ordinates of these camber lines and the values of f and x_f are given in Table I. For any other required value of ΔC_L on a two-dimensional wing, say ΔC_{L_1}, the ordinates of the camber lines in Table I should be multiplied by $\Delta C_{L_1}/1.0$. Similarly, for any other required value of f, the ordinates should be multiplied in proportion.

The corresponding values of $\frac{dz}{dx}$ are given in Table II, having been calculated from equation (30). These values are required when the calculation method is extended to cover thick profiles (Section 5).

It may be noted that $\frac{dz}{dx}$ is infinite at the leading edge for all members of the family of camber lines.

3.2 Sectional aerodynamic characteristics

The flow over a given cambered aerofoil section on a swept wing varies with the spanwise position. Therefore, in addition to f and m, the geometrical parameters φ and y occur in the equations of the sectional aerodynamic characteristics. The parameter y is incorporated in the index n from the original vortex distribution:

$$n = \frac{1}{2}\left(1 - \lambda . \frac{\varphi}{\pi/2}\right)$$

where $\lambda = \lambda(y)$, a function of the spanwise position. n is therefore a function of $\lambda\varphi$.

$0 \leq \lambda \leq 1$ near the centre of a sweptback wing;

$0 \geq \lambda \geq -1$ near the tip of a sweptback wing.

$\lambda(y)$ may be read directly from Fig.1.

3.21 Chordwise loading

The chordwise distributions of vorticity and lift arising from a cambered aerofoil section at an effective incidence α_e are given by equations (28) and (32) respectively:-

$$\gamma_x(x) = 2V_o \sin \pi n \left\{ \alpha_e \left(\frac{1-x}{x}\right)^n + \frac{4.53\ C(m).\ f}{\sin \pi n} \left(\frac{1-x}{x}\right)^m \times \right.$$
$$\left. \left[\frac{1}{\pi m\ (\cot \pi m - \cot \pi n)} - \frac{\sin \pi n}{\sin \pi m} \left(\frac{1}{\pi m\ (\cot \pi m - \cot \pi n)} - 1 \right) \left(\frac{1-x}{x}\right)^{(n-m)} \right] \right\} \quad \ldots\ldots(28)$$

and

$$\Delta C_p(x) = -4 \cos \varphi \left\{ \alpha_e \left(\frac{1-x}{x}\right)^n + \frac{4.53\ C(m).\ f}{\sin \pi n} \left(\frac{1-x}{x}\right)^m \times \right.$$
$$\left. \left[\frac{1}{\pi m\ (\cot \pi m - \cot \pi n)} - \frac{\sin \pi n}{\sin \pi m} \left(\frac{1}{\pi m\ (\cot \pi m - \cot \pi n)} - 1 \right) \left(\frac{1-x}{x}\right)^{(n-m)} \right] \right\} \quad \ldots\ldots(32)$$

The terms due to the camber only are functions of f, x_f, φ and $\lambda(y)$, φ usually occurring in conjunction with λ in the parameter n.

By putting $\varphi = 0$, the distributions on a two-dimensional wing are obtained. Some of these are shown in Fig.5. The distributions range from a constant value when $m = 0$ to a "flat-plate" type of distribution when $m = 1$. On a swept wing the distributions must be calculated from equations (28) and (32) using the appropriate values of λ and φ.

It is interesting to compare the series of camber lines of the present report with the series of NACA mean lines $a = 0$ to $a = 1.0^5$. Both series contain a camber line which gives a constant chordwise distribution of $\Delta C_p(x)$, and in fact the two camber lines are identical. They are characterised by parameters $m = 0$ in the present series and $a = 1.0$ in the NACA series. Other camber lines of the two series do not correspond to each other since they are derived from different types of chordwise loading. In order to obtain a linear loading at the rear of the sections the NACA camber lines have an inflexion near the trailing edge. Elimination of these inflexions introduces a steeper pressure gradient at the point where the loading changes sharply. In the present series of camber lines there are no inflexions.

3.22 Angle of zero lift

The change in the zero lift angle brought about by the camber is denoted by $\Delta\alpha$. Equation (38) shows that it contains f as a factor and that it is also a function of x_f and of $\lambda\varphi$:-

$$\frac{\Delta\alpha}{f} = \frac{4.53\ C(m)}{\pi n \sin \pi m\ (\cot \pi m - \cot \pi n)} \left[\pi n\ (\cot \pi m - \cot \pi n) + 1 - \frac{n}{m} \right] \qquad (38)$$

In Figs.6 and 7 $\frac{\Delta\alpha}{f}$ is plotted against $\lambda\varphi$ for various values of x_f. Therefore for any spanwise position on a swept wing the change in zero lift angle due to camber may be read or interpolated from Figs.6 and 7: no calculation is necessary.

Fig.9 shows the variation of $\frac{\Delta\alpha}{f}$ with position of camber on a two-dimensional wing. The greatest lift increment is obtained when $m = 0$ $(x_f = 0.5)$. This lift increment is nearly 50% greater than that obtained from a circular arc camber line (for which x_f also $= 0.5$). This is because the circular arc has an elliptical chordwise loading whereas the camber line of the present series has a constant loading. In practice, however, much of the extra lift of the constant-load camber line is lost through viscosity effects (see Section 4.11). The camber effect on lift is a minimum when $m = 1$, $(x_f = 0$; see Section 2.32).

The sectional lift coefficient due to camber, ΔC_L, is equal to $\Delta\alpha \times \frac{\partial C_L}{\partial \alpha_e}$. $\frac{\partial C_L}{\partial \alpha_e}$ is given by equation (37):-

$$\frac{\partial C_L}{\partial \alpha_e} = 4\pi n \cdot \frac{\cos \varphi}{\sin \pi n} \qquad (37)$$

Hence ΔC_L may be obtained from $\Delta\alpha$. ΔC_L does not include the induced effects arising from the trailing vortices of the spanwise lift distribution due to camber. For an aerofoil of finite span ΔC_L may be added to the incidence term only if the latter includes these induced effects.

3.23 Pitching moment and centre of pressure

The sectional pitching moment coefficient due to the camber, ΔC_m, is given by equation (41):-

$$\frac{\Delta C_m}{f} = \frac{4.53\ C(m) \cos \varphi}{\sin \pi\ (n-m)} \cdot \left[(2m-1) + (2n-1) \left\{ \pi n\ (\cot \pi m - \cot \pi n) - \frac{n}{m} \right\} \right] \qquad (41)$$

The local centre of pressure position depends on the relative amount of lift contributed by the incidence and camber effects. If the local lift coefficient C_L is known, the C.P. position is given by equation (43):-

$$\Delta x_{C.P.} = -\frac{2n-1}{4} - \frac{C_{m_o}}{C_L} = \frac{\lambda\varphi}{2\pi} - \frac{C_{m_o}}{C_L} \qquad (43)$$

Equation (42) shows that $f \cos \varphi$ is a factor of C_{m_o} and in Fig.8 $\frac{C_{m_o}}{f \cos \varphi}$ is plotted against $\lambda\varphi$ for various positions of camber. Thus C_{m_o} may be read or interpolated from Fig.8 and very little calculation is required to find $\Delta x_{C.P.}$.

Fig.10 shows the variation of the local C.P. position with position of camber on a two-dimensional wing at zero incidence. $x_{C.P.}$ varies from 0.5 for $x_f = 0.5$ $(m=0)$ to 0.25 for $x_f = 0$ $(m=1)$. For a cambered section at incidence the lift force due to incidence acts at 0.25c and so the C.P. position on a two-dimensional wing varies with incidence in the range $0.25 \leqslant x_{C.P.} \leqslant 0.5$.

4 Practical application to thin swept wings of finite aspect ratio

It is now possible to set about the calculation of the chordwise and spanwise loadings of swept wings having thin cambered sections of the type derived in Section 2. Camber lines which are not members of this family must be approximated by the member of the family having the same value of the parameters f and x_f.

Also it is now possible to design wings incorporating camber and twist to have a required chordwise and spanwise loading. The spanwise loading at a given geometric incidence may be given any desired shape by the use of twist alone or camber alone or by an infinite number of combinations of both (provided the flow does not break down anywhere over the aerofoil). However, if the chordwise loadings are also required to be of a definite form, then in general only one of this infinity of combinations of camber, twist and basic incidence will give the required load distribution. Therefore if the complete loading and pressure field over the wing are of interest the camber and twist must be combined in a definite manner and should be matched to each other throughout the span to give the most acceptable distribution. This will usually mean that camber, as well as twist, will vary with the spanwise position and may change from negative camber in one part to positive camber in another. This important point has not been observed in the past, and it is therefore not surprising that up to now cambered wings have not shown the desired benefit when checked experimentally.

It may be pointed out that aerofoil sections expressly designed to have a certain chordwise pressure distribution, e.g. to give a high critical Mach number, should not be applied to swept wings on the basis of their two-dimensional characteristics without examining the effect of the planform on these characteristics, since the improvement in M_{crit} might not be maintained without further modification to camber, twist or thickness distribution.

4.1 Calculation of the loading of a given wing

In the case of a given wing, everything is known about its geometry. The planform is specified which means that φ, λ and n are known everywhere. The geometric incidence α, the camber f, and the position of camber x_f, are also specified everywhere.

4.11 Spanwise loading: general method

The spanwise loading is most conveniently calculated by the method of Ref.2 because the same basic approach is used here as in that method. The description which follows is applicable to wings of about aspect

ratio 3 or greater, provided that the camber and twist do not change rapidly within one chord of the centre-section. If the camber and twist do vary rapidly in this region, the modifications described in Section 4.12 may be applied. The calculation is essentially the same in all cases, however.

In Ref.2 the integral equation of Prandtl is written

$$\frac{2b}{a(\eta) \cdot c(\eta)} \cdot \gamma(\eta) = \alpha(\eta) - \frac{1}{2\pi} \int_{-1}^{+1} \frac{d\gamma(\eta')}{d\eta'} \cdot \frac{d\eta'}{\eta - \eta'} , \qquad (57)$$

(equation (18) of Ref.2),

where $\eta = y \cdot \frac{c(y)}{b/2}$, a non-dimensional spanwise co-ordinate,

$\gamma(\eta)$ = the total non-dimensional vorticity at spanwise position η ,

$$= \frac{\Gamma(\eta)}{b\, V_o} = C_L(\eta) \cdot \frac{c(\eta)}{2b} ,$$

$a(\eta)$ = sectional lift slope,

$c(\eta)$ = local chord,

b = wing-span,

$\alpha(\eta)$ = geometric incidence.

The integral on the right-hand side is then replaced by a finite series in the manner of Multhopp[6] and equation (57) becomes a set of simultaneous equations in γ_ν :-

$$\gamma_\nu \left(b_{\nu\nu} + \frac{2b}{a_\nu\, c_\nu} \right) = \alpha_\nu + \sum_{n=1}^{m}{}' \, b_{\nu n} \cdot \gamma_n \qquad (58)$$

(equation (20) of Ref. 2)

where $\sum_{n=1}^{m}{}'$ means $\sum_{n=1}^{m} b_{\nu n} \cdot \gamma_n - b_{\nu\nu}\, \gamma_\nu$,

and ν is a suffix indicating the pivotal spanwise position.

The coefficients $b_{\nu n}$ and $b_{\nu\nu}$ are given in Ref.2 for the case in which the downwash at the wing is assumed to be half that at infinity. Cases when this assumption is not true are dealt with in Section 4.12. b and c are functions of the planform and the only other quantities which remain to be inserted are the sectional lift slope a_ν and incidence α_ν . As in any other linearised theory it is assumed here that camber and twist do not affect the sectional lift slope which is therefore obtained from the formula

$$a_\nu = a_o \frac{\cos\varphi}{\sin \pi n} \left(1 - \lambda_\nu \cdot \frac{\varphi}{\pi/2}\right) \qquad (59)$$

(see equation (35)), φ being the sweep of the mid-chord line. The incidence α_ν is the total geometric incidence and must include the "equivalent incidence" of the camber at η_ν, i.e. $\Delta\alpha$ of equation (38). It will be noted that equation (38) does not take account of the effect of trailing vortices (i.e. $\Delta\alpha$ is a "sectional characteristic") and so $\Delta\alpha$ does correspond to a geometric incidence and not an effective incidence. Therefore α_ν is, according to our assumptions, the sum of the geometric incidence and $\Delta\alpha$ at η_ν.

The values of Γ_ν are now the only unknowns in (58) and this set of simultaneous equations can be quickly solved by iteration as shown in Ref.2. Thus, from the relation

$$\Gamma_\nu = C_{L_\nu} \cdot \frac{c_\nu}{2b} , \qquad (60)$$

the local lift coefficient may be found at the pivotal spanwise positions. The induced incidence at these positions may also be found from the relations

$$\alpha_{i\nu} = \alpha_\nu - \alpha_{e\nu} = \alpha_\nu - \frac{C_{L_\nu}}{a_\nu} , \qquad (61)$$

since α, C_L and a are now all known at η_ν.

The spanwise loading thus found will only be true at the particular incidence chosen. The loading at any other incidence must be calculated afresh. $\Delta\alpha$ will be the same, since the camber effect is independent of incidence, but the geometric incidence will change by a constant amount over the whole wing. If it is expected that the loading at more than one incidence will be required, it will be much quicker to calculate separately the loading due to the basic incidence, and that due to camber and twist, and then to find the total loading by superposition of these solutions.

For the contribution due to the basic incidence, equation (58) may be divided by α_ν which is constant for all ν :-

$$\frac{\Gamma_\nu}{\alpha_\nu}\left(b_{\nu\nu} + \frac{2b}{a_\nu c_\nu}\right) = 1 + \sum_{n=1}^{m}{}' b_{\nu n} \frac{\Gamma_n}{\alpha_n} \qquad (62)$$

Equation (62) is solved for $\frac{\Gamma_\nu}{\alpha_\nu}$ in exactly the same manner as equation (58). By multiplying by the appropriate value of α_ν, Γ_ν is obtained at the pivotal points for any basic incidence, and thus C_{L_ν} may be found from the relation

$$C_{L_\nu} = \frac{\Gamma_\nu}{\alpha_\nu} \cdot \alpha_\nu \cdot \frac{2b}{c_\nu} .$$

The loading due to camber and twist is constant for all incidences. In this case the incidence inserted in equation (58) for each ν will be the sum of the twist and $\Delta\alpha$ due to the camber at that spanwise position, viz: $\Delta\alpha_{f T_\nu}$. If $\Delta\gamma_\nu$ represents the local circulation due to camber and twist, equation (58) becomes

$$\Delta\gamma_\nu \left(b_{\nu\nu} + \frac{2b}{a_\nu c_\nu} \right) = \Delta\alpha_{fT_\nu} + \sum_{n=1}^{n=m} b_{\nu n} \cdot \Delta\gamma_n \qquad (63)$$

and the local lift coefficient due to camber and twist is given by

$$\Delta C_{L_\nu} = \Delta\gamma_\nu \cdot \frac{2b}{c_\nu} .$$

The total lift coefficient at η_ν may then be found at any incidence by adding the solution of equation (62) for the basic incidence term to the solution of equation (63) for the camber and twist term.

Most of the dimensions and quantities needed to calculate the lift coefficients are obtainable by inspection of the geometry of the wing. Only λ_ν, a_ν and $\Delta\alpha_\nu$ are not obtainable in this way. λ_ν is the value of $\lambda(y)$ at η_ν, and is needed in order to find n_ν, a_ν and $\Delta\alpha_\nu$. λ_ν may be read directly from Fig.1 where it is plotted against y (y is non-dimensional with the local chord). n and a_ν may then be obtained from equations (3) and (59). In practice, however, the more crude interpolation given in Ref.2 is usually adequate:-

$$a(y) = a_s - \lambda(a_s - a_c)$$

where a_s and a_c are the lift slopes at the sheared part and centre section of the wing respectively. Differences between this value and that given by equation (59) lie within the limits of accuracy of the curve of Fig.1, which is an average from experimental data on several sweptback wings. As explained in Section 3.22, $\Delta\alpha_\nu$ may be read directly from Figs.6 and 7.

It is important to note that equation (36), (Section 2.22) is a formula for the "sectional" lift coefficient due to camber. This cannot be used directly to give the spanwise loading due to camber, since it takes no account of the effect of the trailing vortices. The "local" lift coefficient must be calculated as above.

On an aerofoil which has a steep adverse pressure gradient near the trailing edge the boundary layer becomes very thick and may separate. The loss of lift due to viscosity effects is therefore greater than on aerofoils with a more gradual pressure rise. In the present family of camber lines the worst case is the constant-load camber line when $m = 0$ because the theoretical slope of the chordwise loading curve is infinite at the trailing edge. This camber line is identical with the NACA mean line with $a = 1.0$ (see Section 3.21), and the actual zero lift angle of the latter is only 74% of the theoretical value[7]. As the pressure gradient becomes less steep, this percentage rapidly increases. Thus, when calculating aerofoils with a camber line given by m nearly = 0, due allowance should be made for viscosity when estimating $\Delta\alpha$: when

$m = 0$ the theoretical value should be decreased by one-quarter to give the actual $\Delta\alpha$.

$\frac{\Delta\alpha}{f}$ is plotted against $\lambda\varphi$ in Figs.6 and 7. In cases where the centre and tip effects overlap, two values of $\lambda\varphi$ may be obtained at pivotal points near mid-semispan. A mean value should be taken in such cases so that a smooth curve of $\lambda\varphi$ against y is obtained over the whole span. This also applies to the lift slope, a.

Fig.11 shows a comparison between experimental results and the spanwise loading calculated by the above method for a wing of moderate sweepback incorporating camber and twist[8]. Experiment and calculation show good agreement.

The two-dimensional lift slope used in the calculation was corrected for aerofoil thickness and boundary layer effects, the former by a factor $\left(1 + \frac{0.8 \times t/c}{\cos\varphi}\right)$ and the latter by a factor 0.92 (Ref.9) to the thin wing value 2π. This gave a resultant lift slope $a_o = 1.08 \times 2\pi$.

4.12 Spanwise loading special case

An important example is the twisted and cambered wing of Ref.4. This wing was designed[2,4] to have a twist and camber distribution such that, at one fixed $\bar{C}_L$ the chordwise loadings at the centre and at the sheared part were the same, with a constant spanwise loading in between*. Fig.12 shows the sections at the centre and the sheared part.

In common with most wings designed for low Mach numbers and incorporating camber and twist, the centre effect and thus the section modifications extend only over a comparatively short distance from the centre. The spanwise variation of $\Delta\alpha_{fT}$ will be quite similar for any wing designed to have a constant spanwise loading in that region. The modification is zero at $y = 1.0$ and is only 10% of the full modification at $y = 0.5$ (Fig.14). This leads to two difficulties:-

(i) If the usual number of pivotal points is used in the calculation of ΔC_L ($m = 15$, see Ref.2) only two points lie within the cambered and twisted part of the wing and the calculation of ΔC_L is thus inaccurate.

(ii) $\Delta\alpha_{fT}$ changes rapidly in the spanwise direction, which affects the downwash calculation.

To overcome (i) a larger number of pivotal points is required. Alternatively the calculation of ΔC_L can be made for an infinite swept wing; i.e. the tip is assumed to have no influence in the central region of the wing where the camber and twist occur (Ref.2, Appendix II).

Condition (ii) is similar to a rapidly changing twist near the centre section due to rotation effects in the slipstream, or to an upwash from the flow around a body. This problem is dealt with in Ref.10.

---

* That these aims were fully realised has already been reported in Ref.4.

where it was found that a good approximation was obtained by taking the downwash at the wing equal to the downwash at infinity, instead of half that value as is more usual*.

Fig.15 shows the results for the wing being considered. Curve (a) shows the spanwise variation of ΔC_L calculated by the ordinary method of Ref.2 with 15 points. Curve (b) is the calculation for an infinite swept wing, the downwash being assumed to be half that at infinity. This is a straightforward application of Appendix II, 1 of Ref.2 with the points spaced at equal distances of $\frac{1}{4}c$ apart. A similar result would have been obtained by using the ordinary method but increasing the number of points. Curve (c) was calculated by the same procedure as (b) but with the downwash equal to that at infinity. This merely involves multiplying by 2 the coefficients $b_{\nu\nu}$ and $b_{\nu n}$ of Ref.2. By comparison with the experimental values of ΔC_L it is seen that this last method is the most accurate. The difference between curve (b) and the experimental points could not be accounted for by thickness or boundary layer effects: the thickness affects the results by less than 1%, and the boundary layer would need to be considerably greater at the centre than at the sheared part, which is contrary to experimental evidence.

Accordingly, for wings on which the camber and twist vary fairly rapidly within one chord of the centre section, it is recommended that the spanwise loading due to camber and twist be calculated as follows:-

(a) For aspect ratios greater than about 4, such that the tip has no effect in the centre, calculate ΔC_L as for an infinite swept wing using the full value of the downwash at infinity.

(b) For aspect ratios between 3 and 4 such that less than half the pivotal points ($m = 15$) lie within the cambered and twisted region, calculate ΔC_L by the ordinary method of Ref.2 with $m = 31$**, using the full downwash at infinity.

(c) For aspect ratios less than 3, calculate ΔC_L by the ordinary method of Ref.2 with $m = 15$, using the full downwash at infinity. The basic incidence term cannot be calculated directly from Ref.2. An aspect ratio correction is required which will be described in a later note.

The coefficients $b_{\nu\nu}$ and $b_{\nu n}$ used in methods (a), (b) and (c) must be twice those quoted in Refs.2 and 6 in order to give the full downwash effect.

It should be noted that for cases in which the camber and twist are applied to give a constant spanwise loading near the centre the spanwise variation of $\Delta\alpha_{fT}$ will be like that of Fig.14 and the result shown in Fig.15 may be applied directly after multiplying by the ratio of $\Delta\alpha_{fT}$ at the centre sections.

---

* This is, of course, only a crude way of taking account of the fact that that part of the wing which experiences the lift due to the twist has effectively a small aspect ratio. A more detailed discussion of this effect and those connected with small aspect ratio in general will be given in a later note.

** The coefficients $b_{\nu\nu}$ and $b_{\nu n}$ for $m = 31$ and half the downwash at infinity are given in Ref.6.

As Mach number increases, the centre effect decreases more slowly, in a spanwise direction, and the ordinary calculation method should be adequate for wings designed for high M.

4.13 Chordwise loading

To find the chordwise lift distribution it is necessary to know the effective incidence at the particular spanwise position, $\alpha_{e_\nu} = \alpha_\nu - (\alpha_{1\nu} + \Delta\alpha_{1\nu})$, in order to calculate the distribution from equation (32). α_1 and $\Delta\alpha_1$ may be found easily from the spanwise loading calculations already done. All the other parameters are known. It may be convenient to divide $\Delta C_p(x)$ into a component which changes with incidence,

$$[\Delta C_p(x)]_\alpha = -4 \cos\varphi \, (\alpha_\nu - \alpha_{1\nu}) \left(\frac{1-x}{x}\right)^n$$

and a component due to camber which is independent of incidence,

$$[\Delta C_p(x)]_f = -4 \cos\varphi \left\{ -\Delta\alpha_i \left(\frac{1-x}{x}\right)^{n1} + \frac{4.53\, C(m).f}{\sin \pi n} \left(\frac{1-x}{x}\right)^m \times \right.$$

$$\left. \left[\frac{1}{\pi m \,(\cot \pi m - \cot \pi n)} - \frac{\sin \pi n}{\sin \pi m} \left(\frac{1}{\pi m \,(\cot \pi m - \cot \pi n)} - 1 \right) \left(\frac{1-x}{x}\right)^{n-m} \right] \right\}$$

In most cases it will not be necessary to calculate the chordwise distribution at each of the spanwise pivotal points since the distributions at the sheared part, centre and tip will probably be extremes within which the others lie. This may not be so if the wing is twisted in which case a more thorough calculation might be worthwhile.

The local centre of pressure position may easily be found from equation (43) and Fig.8, once the local lift coefficient is known. C_{m_o} may be read or interpolated from Fig.8 and little calculation is involved. Fig.13 shows the variation of the local C.P. position with C_L at the centre section of the wing of Section 4.12. The calculated curve was obtained by the above methods, using the value $x_{C.P.} = 0.24$ for a two-dimensional sheared wing of symmetrical, 12% thick section, and adding $\Delta x_{C.P.}$ to that value.

4.2 The design of a wing with camber and twist

4.21 General procedure

This is the inverse problem to that dealt with in Section 4.1 and on the whole it is a more important application of the calculation method. Camber and twist are to be applied to a wing of given planform so that it will have a certain required loading. For instance, it is possible within the accuracy of the method to design a swept wing having the same chordwise loading everywhere and a constant spanwise loading at a certain $\bar{C}_L$. Consequently, ignoring thickness effects, the isobars are straight up to the centre section and some benefit will be derived at high Mach numbers from this prolongation of the sweep effect. Again, a swept wing may be designed for which the centre and tip effects are eliminated at a certain $\bar{C}_L$, and the load distribution becomes that of the corresponding unswept wing. Thus the stalling characteristics of the swept wing will be similar to those for the unswept wing, with beneficial results in most cases.

The wing planform being given, there are only three variables, the twist, camber and position of camber applied to the basic symmetrical section, i.e. $\Delta\alpha_T$, f and m. The aerodynamic characteristics to be chosen are the spanwise loading, the centre of pressure position and the chordwise loading and when these three conditions are specified the three variables are uniquely determined. If fewer than three conditions are specified, then not all the variables are uniquely determined.

Since the required loadings can be obtained at only one $\bar{C}_L$, this should be specified initially. The spanwise loading may then be chosen (e.g. elliptic) so that the local lift coefficient $(C_{L\alpha} + \Delta C_L)$ is known at all spanwise positions. The equations of Ref.2 for the spanwise loading are now

$$(\gamma_{\nu_\alpha} + \Delta\gamma_\nu)\left(b_{\nu\nu} + \frac{2b}{a_\nu c_\nu}\right) = [\alpha_\nu + \Delta\alpha_{fT_\nu}] + \sum_{n=1}^{m} b_{\nu n}(\gamma_{n_\alpha} + \Delta\gamma_n),$$

where α_ν is the geometric incidence of the basic section. The only unknown in this equation is $[\alpha_\nu + \Delta\alpha_{fT_\nu}]$ which can therefore be determined at the spanwise pivotal points*.

The required spanwise loading can be achieved entirely by camber or entirely by twist or by a combination of both, none of the variables $\Delta\alpha_T$, m or f being uniquely determined. The only stipulation is that $\Delta\alpha + [\alpha + \Delta\alpha_T] =$ the required $[\alpha + \Delta\alpha_{fT}]$ at any spanwise position. $[\alpha + \Delta\alpha_T]$ is the new geometric incidence. For any m and f, $\Delta\alpha$ may be read or interpolated from Figs.6 and 7.

Fig.16 shows as an illustration the spanwise loading of a tapered wing of 35° sweep, for which $\gamma_{\nu_\alpha} + \Delta\gamma_\nu$ was chosen to be the same as on the corresponding unswept wing at $\bar{C}_L = 1.0$. Curve (a) of Fig.17 shows the amount of twist alone necessary to achieve this loading**. Fig.16 also shows the modified spanwise distributions at other values of $\bar{C}_L$.

If in addition to the spanwise loading the centre of pressure position is specified, a further relationship between the camber and twist is introduced. Equations (42) and (43) give

$$\Delta x_{C.P.} = \frac{\lambda\varphi}{2\pi} + \frac{1}{C_L} \cdot \frac{9.06 \cdot C(m) \cdot f \cdot \cos\varphi \cdot (m-n)}{\sin\pi(m-n)} \qquad (64)$$

Hence for a particular value of C_L, the required $\Delta x_{C.P.}$ establishes a connection between m and f. Either m or f is a free choice. There are still an infinite number of combinations of m and f, each combination giving rise to a certain $\Delta\alpha$ (obtainable from Figs.6 and 7) and therefore determining $[\alpha + \alpha_T]$.

---

* The considerations of Section 4.12 still apply, and a modified loading equation should be used if necessary.

** The basic incidence was taken as that at the sheared part of the wing.

If now the chordwise loading is specified, a third equation connects the three variables $\Delta\alpha_{fT}$, m and f, and they are uniquely determined*. This equation is (32), in which α_e, the effective incidence, is the difference between the geometric incidence (including the twist) and the induced incidence based on the chosen spanwise loading. The chordwise loading is not a purely arbitrary choice, since it must be of a form which can be realised by a cambered section of the present series at incidence. Several camber lines may be superimposed if necessary, in which case

$$\alpha + \Delta\alpha_T + \Sigma\,\Delta\alpha = \alpha + \Delta\alpha_{fT} ,$$

$$\Delta x_{C.P.} = \frac{\lambda\varphi}{2\pi} + \frac{1}{C_L}\,\Sigma\,\frac{9.06\ C(m).f.\cos\varphi.(m-n)}{\sin\pi(m-n)} , \text{ etc.}$$

Curves (b) and (c) of Fig.17 show the amount of camber and twist necessary to give a "two-dimensional flat-plate" type of chordwise loading throughout the span at $\bar{C}_L = 1.0$ and $\bar{C}_L = 0.2$, while maintaining the spanwise loading of Fig.16. In this case, m = 0.5.

Modification of an aerofoil section by camber and twist alone will not generally be sufficient to give a specified chordwise pressure distribution (as distinct from chordwise lift distribution) on the surface of a thick aerofoil. Modifications to the thickness distribution of the section are necessary[11], and the calculation of these is outside the scope of this report. However the effect of thickness in a given cambered aerofoil is considered in Section 5.

4.22 Connection between the chordwise loadings at different spanwise positions

Although the chordwise loadings at different spanwise positions on an aerofoil may be chosen independently of each other, it will often be the case that a direct relationship is required between them. In such a case the required camber and twist may be found by using this relationship in the appropriate formulae.

For example, consider a wing swept at an angle φ, the basic section of which is taken to be that at the sheared part. Let the required relationship be that the chordwise loading is the same at all spanwise positions between the centre and the sheared part (i.e. $0 \leqslant \lambda \leqslant 1$). If the basic section has a camber line with parameters m_s and f_s, at an effective incidence $[\alpha_e]_s$, then the chordwise loading at the sheared part is given by equations (31) and (6) as

$$[\Delta C_p(x)]_s = -4\cos\varphi\left\{A_1\left(\frac{1-x}{x}\right)^{\frac{1}{2}} + A_2\left(\frac{1-x}{x}\right)^{m_s}\right\}$$

---

* If the chordwise loading is chosen after the spanwise loading, both m and f are determined simultaneously and the centre of pressure is then necessarily fixed.

At any spanwise position denoted by $\lambda = \lambda_1$, $(n=n_1)$,

$$[\gamma_x(x)]_{\lambda_1} = -\frac{V_o}{2} \cdot \frac{1}{[\cos \varphi_v]_{\lambda_1}} \cdot [\Delta C_p(x)]_{\lambda_1}$$

$$= -\frac{V_o}{2} \cdot \frac{1}{[\cos \varphi_v]_{\lambda_1}} \cdot [\Delta C_p(x)]_s$$

in accordance with the required condition.

Substituting this value of $[\gamma_x(x)]_{\lambda_1}$ in equations (7) and (15),

$$[\alpha_e]_{\lambda_1} + \frac{dz}{dx} = \frac{v_z}{V_o}$$

$$= A_1 \cdot \frac{\cos \varphi}{[\cos \varphi_v]_{\lambda_1}} \cdot \left\{1 + \cot \pi n_1 \left(\frac{1-x}{x}\right)^{\frac{1}{2}}\right\}$$

$$+ A_2 \cdot \frac{\cos \varphi}{[\cos \varphi_v]_{\lambda_1}} \cdot \left\{\frac{1}{\sin \pi m_s} - (\cot \pi m_s - \cot \pi n_1)\left(\frac{1-x}{x}\right)^{m_s}\right\}$$

Integrating with respect to x, and noting that $z=0$ at $x=0$ and $x=1$,

$$[z]_{\lambda_1} = \frac{\cos \varphi}{[\cos \varphi_v]_{\lambda_1}} \left[\frac{1}{2} A_1 \cot \pi n_1 \left\{\frac{\pi}{2}(1-2x) - \sin^{-1}(1-2x) + \sqrt{1-(1-2x)^2}\right\}\right.$$

$$\left. + A_2(\cot \pi m_s - \cot \pi n_1)\left\{\frac{\pi m_s}{\sin \pi m_s} x - \int_o^x \left(\frac{1-x}{x}\right)^{m_s} dx\right\}\right]$$

and

$$[\alpha_e]_{\lambda_1} = A_1 \frac{\cos \varphi}{[\cos \varphi_v]_{\lambda_1}} \left(1 + \frac{\pi}{2} \cot \pi n_1\right)$$

$$+ A_2 \frac{\cos \varphi}{[\cos \varphi_v]_{\lambda_1}} \cdot \frac{1}{\sin \pi m_s} \left\{1 - \pi m_s(\cot \pi m_s - \cot \pi n_1)\right\} \qquad (65)$$

But $z_s = A_2 \cot \pi m_s \left\{\frac{\pi m_s}{\sin \pi m_s} x - \int_o^x \left(\frac{1-x}{x}\right)^{m_s} dx\right\}$, from equation (21).

Therefore $[z]_{\lambda_1} = \frac{\cos \varphi}{[\cos \varphi_v]_{\lambda_1}} \cdot (1 - \tan \pi m_s \cot \pi n_1) \cdot z_s$

$$+ A_1 \frac{1}{2 \tan \pi n_1} \cdot \frac{\cos \varphi}{[\cos \varphi_v]_{\lambda_1}} \left\{\frac{\pi}{2}(1-2x) - \sin^{-1}(1-2x) + \sqrt{1-(1-2x)^2}\right\} \qquad (66)$$

Applying equations (20) and (22) at the sheared part, A_1 may be eliminated from (65) and (66):-

$$[z]_{\lambda_1} = \frac{\cos\varphi}{[\cos\varphi_v]_{\lambda_1}} \cdot (1 - \tan\pi m_s \cdot \cot\pi n_1) \cdot z_s$$

$$+ \frac{1}{2\tan\pi n_1} \cdot \frac{\cos\varphi}{[\cos\varphi_v]_{\lambda_1}} \cdot \left[\left\{[\alpha_e]_s - \frac{4.53\, C(m_s) \cdot f_s}{\pi m_s \cdot \cos\pi m_s}(1-\pi m_s \cot\pi m_s)\right\}\times\right.$$

$$\left.\left\{\frac{\pi}{2}(1-2x) - \sin^{-1}(1-2x) + \sqrt{1-(1-2x)^2}\right\}\right] \qquad (67)$$

and

$$[\alpha_e]_{\lambda_1} = \frac{\cos\varphi}{[\cos\varphi_v]_{\lambda_1}} \left(1 + \frac{\pi}{2}\cot\pi n_1\right) \cdot [\alpha_e]_s$$

$$+ \frac{4.53\, C(m_s) \cdot f_s}{\cos\pi m_s} \cdot \frac{1}{2\tan\pi n_1} \cdot \frac{\cos\varphi}{[\cos\varphi_v]_{\lambda_1}} \cdot \left(\pi\cot\pi m_s + 2 - \frac{1}{m_s}\right)$$

(68)

$[z]_{\lambda_1}$ and $[\alpha_e]_{\lambda_1}$ are the camber line and effective incidence required at the spanwise position denoted by $\lambda = \lambda_1$ for the chordwise loading there to be the same as that at the sheared part. Equation (67) shows that in general the required camber line is a combination of that at the sheared part and that defined by m = 0.5. The latter is of the form:-

$$\text{constant} \times \left[\frac{\pi}{2}(1-2x) - \sin^{-1}(1-2x) + \sqrt{1-(1-2x)^2}\right]$$

The geometric twist at $\lambda = \lambda_1$ is $[\alpha_e + \alpha_1]_{\lambda_1} - [\alpha_e + \alpha_1]_s$.

Two particular cases may be noted:-

(a) If a flat-plate distribution is required at all spanwise positions, m = 1 at the sheared part (i.e. $A_2 = 0$) and the vortex distribution is

$$\gamma_x(x) = 2 V_o [\alpha_e]_s \left(\frac{1-x}{x}\right)^{\frac{1}{2}} \qquad \text{(see Section 2.32).}$$

[N.B. $m = \frac{1}{2}$, which appears to give a flat-plate distribution, is the case mentioned in Section 2.33, i.e. m=n.]

Then

$$[z]_{\lambda_1} = \frac{1}{2\tan\pi n_1} \cdot \frac{\cos\varphi}{[\cos\varphi_v]_{\lambda_1}} \cdot [\alpha_e]_s \cdot \left[\frac{\pi}{2}(1-2x) - \sin^{-1}(1-2x) + \sqrt{1-(1-2x)^2}\right]$$

and

$$[\alpha_e]_{\lambda_1} = \frac{\cos\varphi}{[\cos\varphi_v]_{\lambda_1}} \cdot \left(1 + \frac{\pi}{2}\tan\varphi\right) \cdot [\alpha_e]_s ,$$

from equations (67) and (68). $[z]_{\lambda_1}$ is positive, therefore the camber is negative (see Section 2.13).

Thus a symmetrical section at the sheared part requires a camber line at other positions given by m = 0.5, plus a certain twist, in order to obtain a "flat-plate" chordwise loading everywhere.

(b) If a constant chordwise loading is required at all spanwise positions (i.e. $C_p(x)$ = const.) then at the sheared part m = 0. Thus $A_1 = 0$, (i.e. $[\alpha_e]_s = 0$) and

$$\gamma_x(x) = 2 V_o \cdot A_2$$

at the sheared part, with $n = \frac{1}{2}$.

At $\lambda = \lambda_1$ this gives a camber shape

$$[z]_{\lambda_1} = \frac{\cos \varphi}{[\cos \varphi_v]_{\lambda_1}} \cdot z_s$$

and

$$[\alpha_e]_{\lambda_1} = \frac{4.53}{\tan \pi n_1} \cdot \frac{\cos \varphi}{[\cos \varphi_v]_{\lambda_1}} \cdot f_s.$$

This means that no camber line of the shape defined by m = 0.5 is required: the desired loading is obtained simply by reducing the amount of the original camber at the sheared part and imparting a twist. This should simplify the merging of the section shapes along the span.

5 Pressure distributions on thick cambered aerofoils

So far the treatment has been confined to thin cambered and twisted aerofoils. For thick wings this gives only a first approximation to $\Delta C_p(x)$, and no information about the pressure distribution on the surface. One object of incorporating camber and twist is to increase the critical Mach number by reducing suction peaks or straightening isobars and to do this the pressure distribution must be known. Again, on swept wings the effect of thickness is more important than on unswept wings, since the effective thickness-chord ratio is $\frac{t/c}{\cos \varphi}^3$.

The method of Ref.3, extended to cover all spanwise positions can be used to calculate the pressure distribution over thick cambered aerofoils. This gives the following results:-

For the sheared part of the wing,

$$C_p(x) = 1 - \cos^2 \alpha_e \cdot \sin^2 \varphi - \frac{a_n^2}{a_n^2 + \left(\frac{B_n - D_n}{\cos \varphi}\right)^2} \times$$

$$\left\{\cos \alpha_e \left[\cos \varphi \left(1 - \frac{A_n}{a_n \cos \varphi}\right) \pm \frac{\Delta\gamma_x(x)}{2 V_o}\right]\right.$$

$$\left. \pm \sin \alpha_e \sqrt{\frac{1-x}{x}} \left(1 + \frac{G_n}{\cos \varphi}\right)\right\}^2 .$$

For the centre of a swept wing,

$$C_p(x) = 1 - \frac{a_n^2}{a_n^2 + (B_n - D_n)^2} \times$$

$$\left\{\cos \alpha_e \left[1 - \frac{\cos \varphi}{a_n} (A_n + f(\varphi) \cdot B_n) \pm \frac{\Delta\gamma_x(x)}{2 V_o}\right]\right.$$

$$\left. \pm \sin \alpha_e \cdot \cos \varphi \cdot \left(\frac{1-x}{x}\right)^{n(\varphi,0)} \left(1 + \frac{G_n}{\cos \varphi}\right)\right\}^2 .$$

For any intermediate position between the centre and sheared part, or between sheared part and tip,

$$C_p(x) = 1 - \frac{a_n^2}{a_n^2 + \left(\frac{B_n - D_n}{\cos [(1 - |\mu|) \varphi]}\right)^2} \times$$

$$\left[\left\{\cos \alpha_e \left(1 - \kappa \cos \varphi \cdot \frac{A_n}{a_n} - \mu \cdot \cos \varphi \cdot f(\varphi) \cdot \frac{B_n}{a_n} \pm \cos \varphi_V \cdot \frac{\Delta\gamma_x(x)}{2 V_o}\right)\right.\right.$$

$$\left.\left. \pm \sin \alpha_e \cdot \cos \varphi_V \cdot \sin \pi n(\varphi,y) \cdot \left(\frac{1-x}{x}\right)^{n(\varphi,y)} \left(1 + \frac{G_n}{\cos \varphi}\right)\right\}^2\right.$$

$$+ \left\{\cos \alpha_e \left[-(1-\mu) \sin \varphi \cdot \frac{A_n}{a_n} \pm \sin \varphi_V \cdot \frac{\Delta\gamma_x(x)}{2 V_o}\right]\right.$$

$$\left. \pm \sin \alpha_e \sin \varphi_V \sin \pi n(\varphi,y) \cdot \left(\frac{1-x}{x}\right)^{n(\varphi,y)} \left(1 + \frac{G_n}{\cos \varphi}\right)\right\}^2$$

$$\left. + (1 - \mu^2) \cos^2 \alpha_e \sin^2 \varphi \left(\frac{B_n - D_n}{a_n \cos [(1-\mu) \varphi]}\right)^2\right] .$$

In the above equations, the camber terms C_o and C_n of Ref.3 have been replaced by $\Delta\gamma_x(x)$, the chordwise vortex distribution due to camber, i.e. the second term in equation (28). However C_o and C_n contain the co-ordinates of the camber line and can be used in the equations if desired.

The terms A_n, etc., are the sums $\sum_{m=1}^{N-1} A_{mn} \cdot 2 z_{tm}$, etc.

It is usually good enough for the sweep angle, φ, to have the same value throughout, namely the sweep of the mid-chord line. α_e, $\gamma_x(x)$, $n(\varphi,y)$ and λ have the values appropriate to the spanwise position. The suffix n denotes the chordwise pivotal point.

$f(\varphi)$, $\kappa(y)$, and $\mu(y)$ are functions of the planform:

$$f(\varphi) = -\frac{1}{\pi} \cdot \log \frac{1 - \sin \varphi}{1 + \sin \varphi}$$

$\kappa(y)$, $\mu(y)_{centre}$ and $\mu(y)_{tip}$ are plotted in Fig.1 and may be read off directly. $\kappa = 1$, except near the tip.

a_n, A_{mn}, B_{mn}, D_{mn}, G_{mn} are coefficients which are tabulated in Ref.3 along with the abscissae of the chordwise pivotal points.

Fig.18 shows the kind of aerofoil section which can be obtained in practice. Three 10% profiles were constructed by superimposing the thickness distribution of the RAE 104 profile on three camber lines of the family with positions of camber at $x_f = 0$, 0.288 and 0.5, (i.e. $m = 1.0$, 0.5 and 0.)

Figs.19 and 20 show the chordwise pressure and lift distributions calculated by the above method for three two-dimensional wings having these aerofoil sections. From Fig.19 it can be seen that the camber line defined by $m = 0$ does not in fact give a constant chordwise loading when thickness effects are considered, but the difference is not very great. The thickness effect is similar for $m = 0.5$.

The various types of pressure distribution on the surface are shown in Fig.20. The curves for $m = 0$ and $m = 1.0$ (a symmetrical section at incidence) are extremes within which the others will lie.

Nomenclature

a	lift slope
b	wing span
$b_{\nu\nu}$, $b_{\nu n}$	coefficients, tabulated in Ref.6
c	chord
f	Camber: i.e. maximum z ordinate, dimensionless with chord
$x_{C.P.}$	chordwise position of centre of pressure
$\Delta x_{C.P.}$	change in centre of pressure position compared with two-dimensional wing of symmetrical section
m	a function of the position of camber, x_f
$n(\varphi,y)$	a function of the wing geometry
t/c	thickness-chord ratio

Nomenclature (Contd)

v_z	downwash velocity at the aerofoil
V_x, V_z	x- and z-components of velocity V
V_o	free stream velocity
x y,z	co-ordinates as defined in F g 2 dimensionless with the local chord
x_f	position of camber dimensionless with local chord
A_1 A_2	coefficients in the chordwise vortex distribution
$B(x,m)$	$= \int_0^x \left(\frac{1-x'}{x'}\right)^m dx - x\left(\frac{1-x}{x}\right)^m$
	$= \int_s^\infty \frac{d\omega'}{1 + s'^{1/m}}$, where $s, \omega' = \left(\frac{1-x}{x}\right)^m, \left(\frac{1-x'}{x'}\right)^m$
$C(m)$	$= \frac{\pi m}{4\ 53\ B(x_f,m)}$, a function of m
a_n, A_n B_n, C_n D_n, G_n	coefficients given in Ref 3
X	co-ordinate perpendicular to vortex filaments
α	geometric incidence
α_i	induced incidence
α_e	effective incidence
	= geometric incidence - total induced incidence
$\Delta\alpha$	equivalent change of incidence due to camber
$\Delta\alpha_i$	induced incidence arising from camber lift distribution
$\Delta\alpha_T$	twist
$\Delta\alpha_{f\,T}$	$= \Delta\alpha + \Delta\alpha_T$
$\gamma_x(x)$	distribution of vorticity per unit area along the chordline
Γ	total vorticity per unit span at any spanwise position
γ	$= \frac{\Gamma}{b\ V_o}$, total non-dimensional vorticity per unit span at any spanwise position
$\Delta\gamma$	total non-dimensional vorticity due to camber

Nomenclature (Contd.)

η	spanwise co-ordinate, dimensionless with semi-span
$\lambda(y)$	a function of the spanwise position
$\sigma(\varphi,y)$	a function of the wing geometry
φ	angle of sweep
φ_v	angle of sweep of a vortex filament
$f(\varphi), \kappa(y)$ $\mu(y)_{centre}$, $\kappa(y) \times \mu(y)_{tip}$	functions of the wing geometry
$C_p(x)$	pressure coefficient
$\Delta C_p(x)$	difference between pressure coefficients on upper and lower surfaces
C_L	sectional, local — lift coefficient
$\bar{C}_L$	total lift coefficient of aerofoil
ΔC_L	sectional, local — lift coefficient due to camber
C_m	sectional, local — pitching moment coefficient
C_{m_o}	" " " " at zero lift
ΔC_m	sectional, local — pitching moment coefficient due to camber

Suffices

α	due to incidence
e	effective
i	induced
f	due to camber
n	denotes chordwise pivotal points
ν	denotes spanwise pivotal points
λ_1	at a spanwise position where $\lambda = \lambda_1$
s	at the sheared part
T	due to twist
x	distributed on the x-axis
U.S.	upper surface
L.S.	lower surface

REFERENCES

No.	Author	Title, etc.
1	G.M. Roper	Calculation of the effect of camber and twist on the pressure distribution and drag on some curved plates at supersonic speeds. R.A.E. Report No. Aero 2386, 1950. A.R.C. No. 13,755
2	D. Küchemann	A simple method for calculating the span and chordwise loadings on thin swept wings. R.A.E. Report No. Aero 2392, 1950. A.R.C. No. 13,758
3	J. Weber	A simple method for calculating the chordwise pressure distribution on two-dimensional and swept wings for aerofoil sections of finite thickness. R.A.E. Report No. Aero 2391, 1950. A.R.C. No. 13,757
4	J. Weber and G.G. Brebner	Low speed tests on 45° sweptback wings: Part I. Pressure measurements on wings of aspect ratio 5. R.A.E. Report No. Aero 2374, 1950. A.R.C. No. 13,655
5	I.H. Abbott, A.E. von Doenhoff and L.S. Stivers,	Summary of airfoil data, Part II. NACA/TIB/1201, 1945.
6	H. Multhopp	Die Berechnung der Auftriebsverteilung von Tragflügeln. Luftfahrtforschung, vol.15, 1938, p.153. Translated in A.R.C. No.8516.
7	L.K. Loftin	Theoretical and experimental data for a number of NACA 6A-Series airfoil sections. NACA Report 903, 1948.
8	D.J. Kettle	24 ft wind tunnel tests on the G.A. V wing tailless glider; Part II. Pressure distribution measurements. R.A.E. Report No. Aero 2147, 1946. A.R.C. No. 10,144
9	G.G. Brebner and J.A. Bagley	Boundary layer and pressure measurements on a two-dimensional wing at low speed. R.A.E. Report No. Aero 2455, 1952. A.R.C. No. 15,083
10	I. Ginzel	Die auftriebsverteilung eines triefen verwundenen rechteckflügels. Jahrbuch 1940 d. Deutschen Luftfahrtforschung, I, p.238. M.O.S. Monograph. AVA F1.2, R and T.1024, 1947.
11	D. Küchemann	Wing junction, fuselage and nacelles for sweptback wings. R.A.E. Report No. Aero 2219, 1947. A.R.C. No. 11,035

TABLE I

Co-ordinates of camber lines which give $\Delta C_L = 1.0$ on a two-dimensional unswept wing at $\alpha_e = 0$ (Fig.4)

z

x/c \ m	0	0.1	0.2	0.3	0.4	0.5
0.01	0.0045	0.0065	0.0097	0.0144	0.0214	0.0314
0.05	0.0158	0.0215	0.0291	0.0385	0.0494	0.0623
0.10	0.0259	0.0338	0.0435	0.0545	0.0665	0.0794
0.20	0.0398	0.0498	0.0606	0.0718	0.0829	0.0938
0.30	0.0486	0.0589	0.0693	0.0793	0.0885	0.0967
0.40	0.0536	0.0631	0.0723	0.0806	0.0876	0.0933
0.50	0.0552	0.0635	0.0709	0.0772	0.0820	0.0854
0.60	0.0536	0.0603	0.0657	0.0699	0.0727	0.0740
0.70	0.0486	0.0534	0.0567	0.0588	0.0598	0.0597
0.80	0.0398	0.0423	0.0437	0.0442	0.0438	0.0427
0.90	0.0259	0.0264	0.0262	0.0255	0.0244	0.0231
1.00	0	0	0	0	0	0
x_f	0.500	0.459	0.417	0.375	0.332	0.288
f	0.0552	0.0638	0.0723	0.0806	0.0888	0.0968

z

x/c \ m	0.5	0.6	0.7	0.8	0.9	1.0
0.01	0.0314	0.0451	0.0635	0.0876	0.1187	0.1576
0.05	0.0623	0.0773	0.0943	0.1131	0.1327	0.1512
0.10	0.0794	0.0932	0.1072	0.1207	0.1333	0.1432
0.20	0.0938	0.1039	0.1128	0.1202	0.1254	0.1273
0.30	0.0967	0.1035	0.1086	0.1119	0.1131	0.1114
0.40	0.0933	0.0973	0.0995	0.1001	0.0989	0.0955
0.50	0.0854	0.0871	0.0873	0.0862	0.0837	0.0796
0.60	0.0740	0.0740	0.0729	0.0709	0.0678	0.0637
0.70	0.0597	0.0586	0.0568	0.0544	0.0514	0.0477
0.80	0.0427	0.0411	0.0392	0.0370	0.0346	0.0318
0.90	0.0231	0.0216	0.0202	0.0188	0.0174	0.0159
1.00	0	0	0	0	0	0
x_f	0.288	0.242	0.193	0.140	0.079	0
f	0.0968	0.1046	0.1128	0.1220	0.1337	0.1592

TABLE II

Slopes of the camber lines in Table I and Fig.4

$\frac{dz}{dx}$

x/c \ m	0	0.1	0.2	0.3	0.4	0.5
0	$-\infty$	$-\infty$	$-\infty$	$-\infty$	$-\infty$	$-\infty$
0.01	-0.366	-0.516	-0.699	-0.921	-1.172	-1.428
0.05	-0.236	-0.296	-0.356	-0.412	-0.455	-0.475
0.10	-0.175	-0.208	-0.235	-0.252	-0.257	-0.244
0.20	-0.110	-0.120	-0.122	-0.115	-0.099	-0.073
0.30	-0.067	-0.065	-0.056	-0.040	-0.019	+0.007
0.40	-0.032	-0.022	-0.007	+0.012	+0.034	0.059
0.50	0	+0.015	+0.033	0.054	0.076	0.097
0.60	+0.032	0.051	0.071	0.092	0.111	0.129
0.70	0.067	0.089	0.109	0.128	0.144	0.156
0.80	0.110	0.133	0.151	0.166	0.177	0.183
0.90	0.175	0.194	0.207	0.213	0.214	0.211
1.00	∞	0.922	0.520	0.383	0.312	0.268
x_f	0.500	0.459	0.417	0.375	0.332	0.288
f	0.0552	0.0638	0.0723	0.0806	0.0888	0.0968

$\frac{dz}{dx}$

x/c \ m	0.5	0.6	0.7	0.8	0.9	1.0
0	$-\infty$	$-\infty$	$-\infty$	$-\infty$	$-\infty$	+0.159
0.01	-1.428	-1.644	-1.735	-1.585	-1.025	+0.159
0.05	-0.475	-0.462	-0.401	-0.281	-0.096	0.159
0.10	-0.244	-0.209	-0.151	-0.069	+0.037	0.159
0.20	-0.073	-0.038	+0.006	+0.056	0.109	0.159
0.30	+0.007	+0.038	0.071	0.104	0.134	0.159
0.40	0.059	0.084	0.108	0.130	0.148	0.159
0.50	0.097	0.117	0.134	0.147	0.156	0.159
0.60	0.129	0.143	0.153	0.160	0.162	0.159
0.70	0.156	0.165	0.169	0.170	0.167	0.159
0.80	0.183	0.185	0.183	0.178	0.170	0.159
0.90	0.211	0.205	0.196	0.185	0.173	0.159
1.00	0.268	0.237	0.212	0.193	0.176	0.159
x_f	0.288	0.242	0.193	0.140	0.079	0
f	0.0968	0.1046	0.1128	0.1220	0.1337	0.1592

Wt.2078.CP171.K3. Printed in Great Britain.

FIG.I.

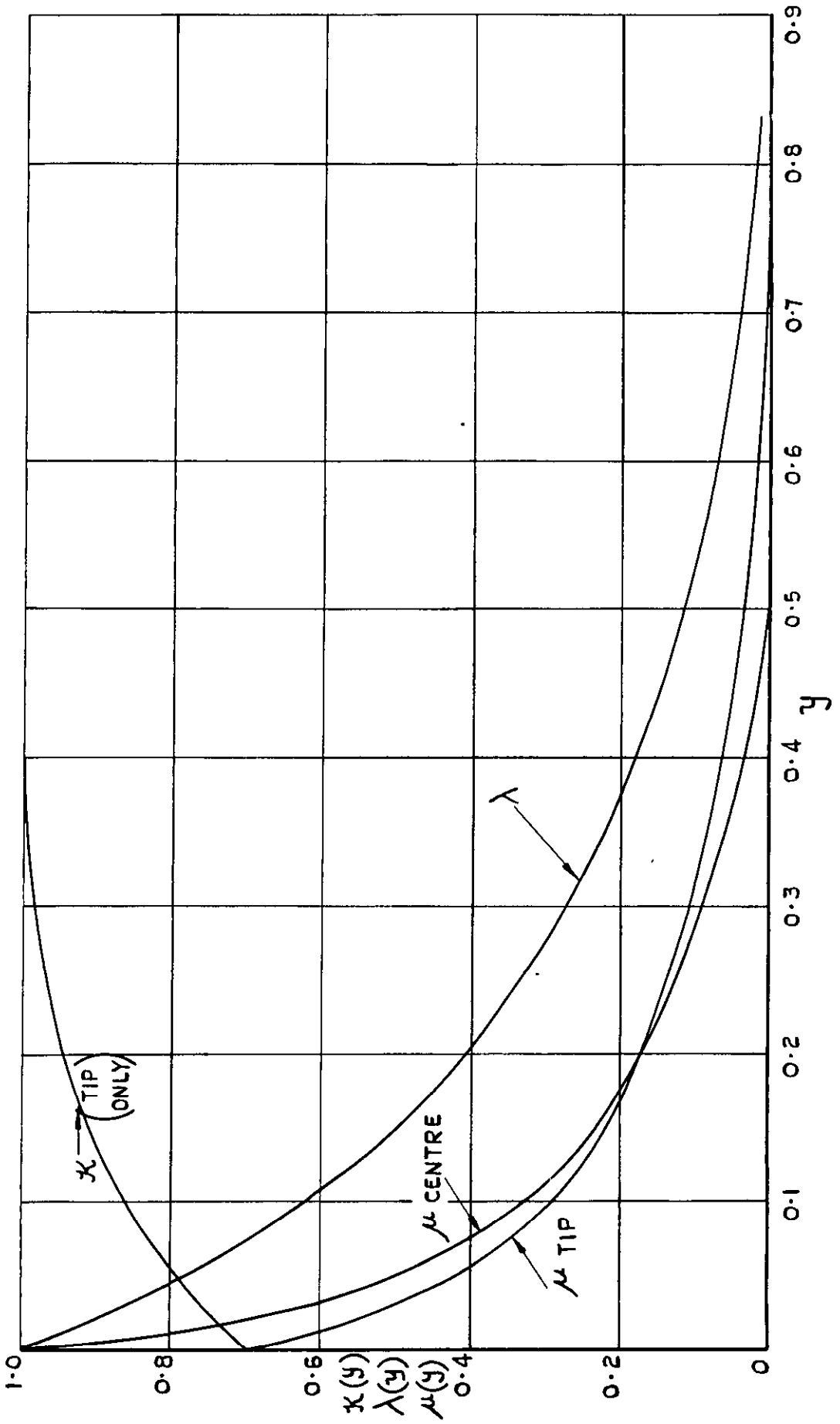

FIG.I. SPANWISE VARIATION OF λ, κ AND μ.

(SEE REF. 2, FIG.I.)

FIG. 2 & 3.

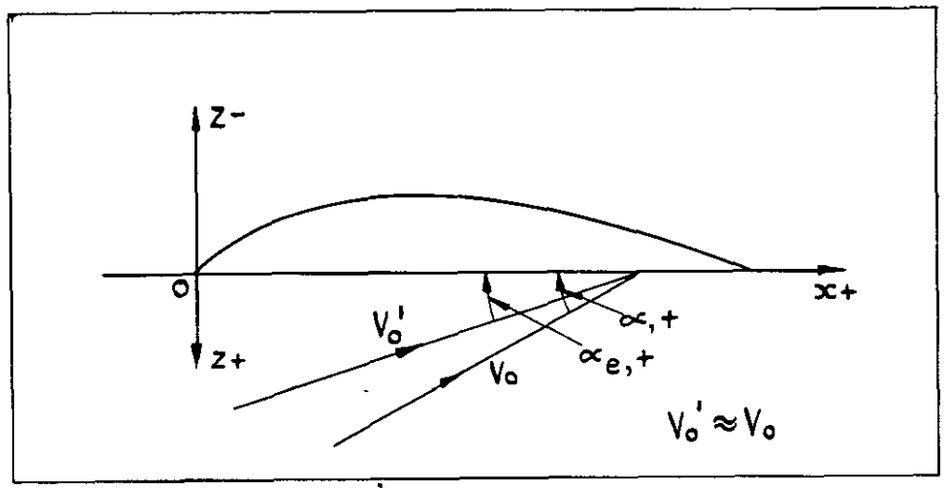

FIG. 2. CAMBER LINE AND REFERENCE AXES.

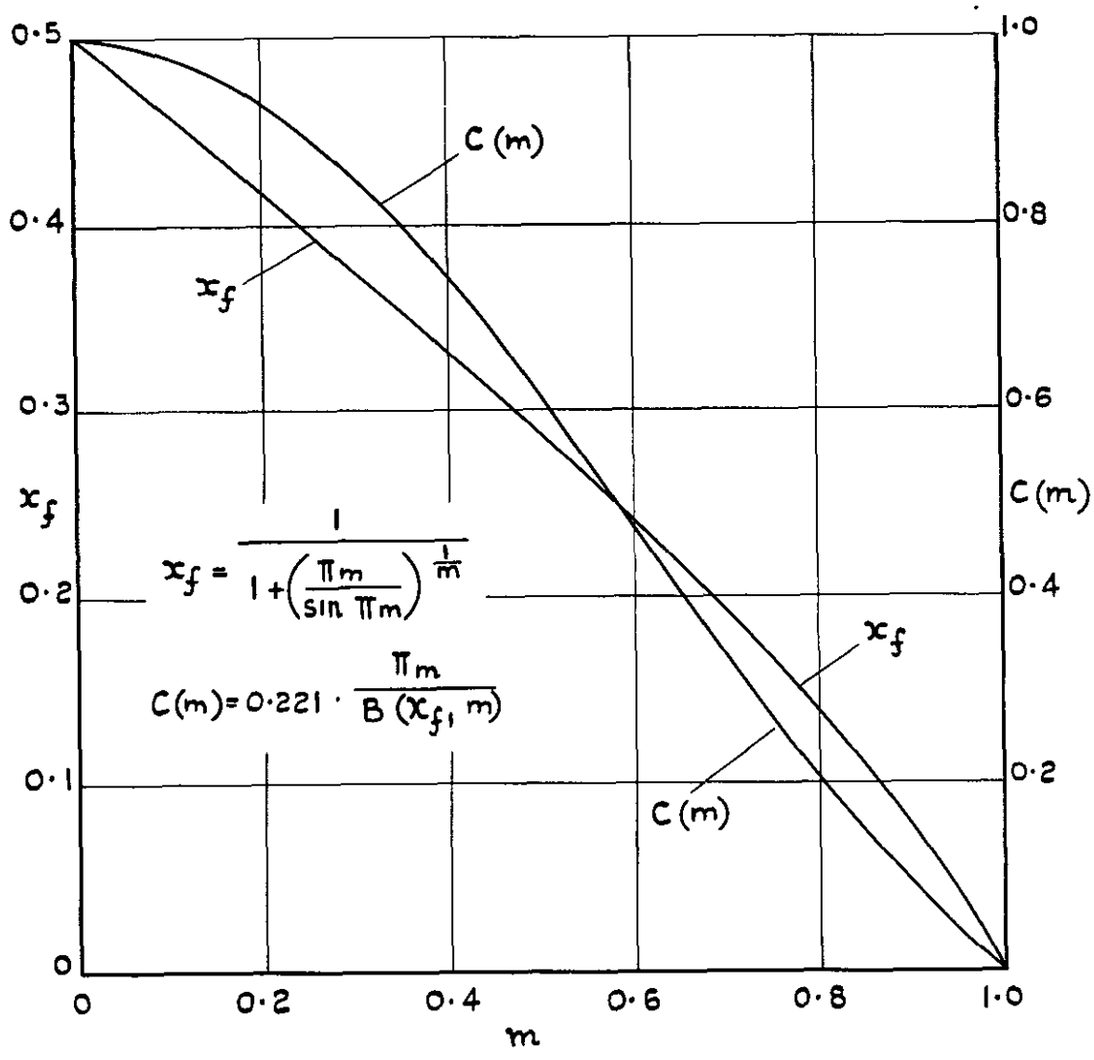

FIG. 3. TWO FUNCTIONS OF m.

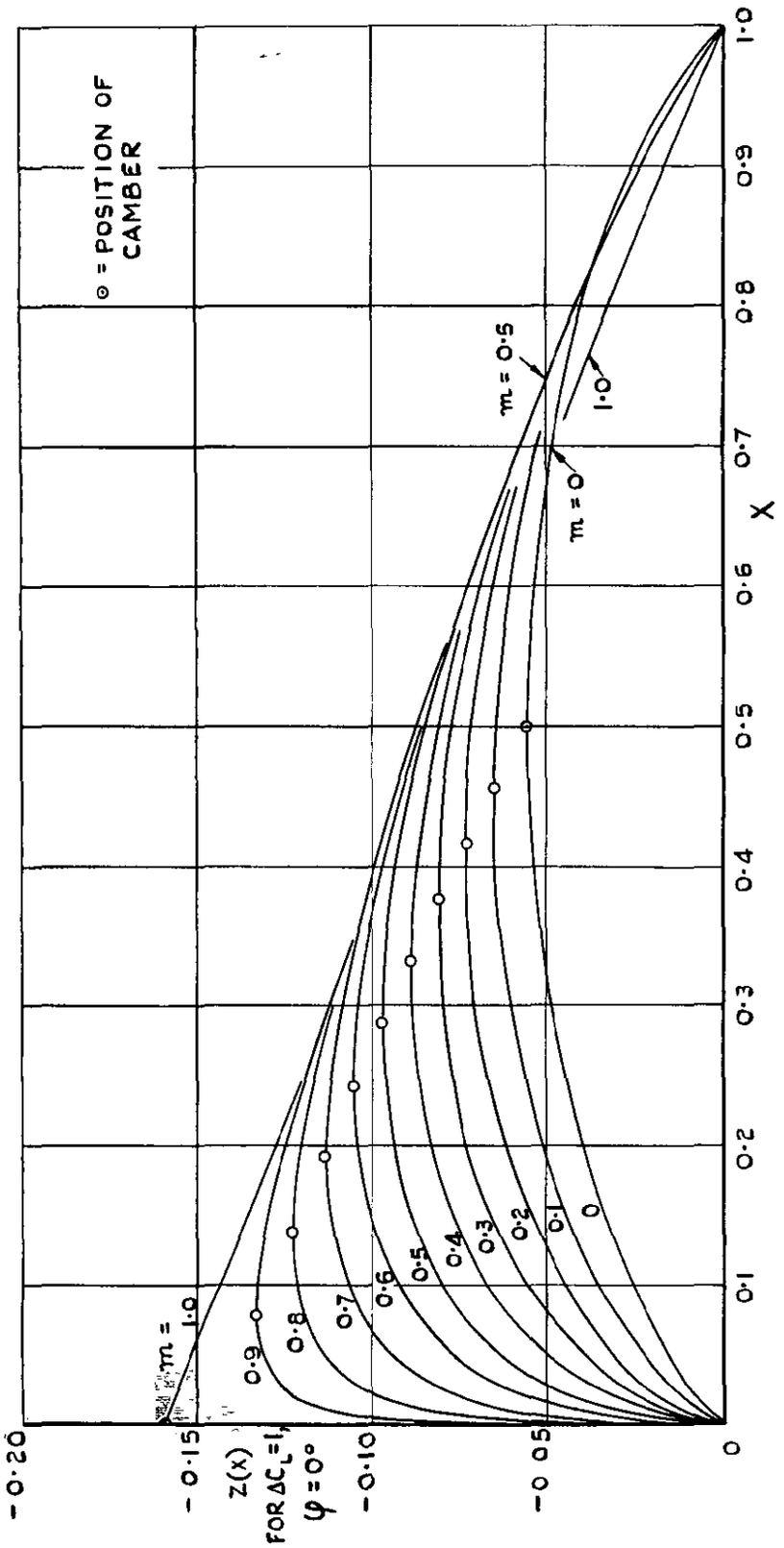

FIG. 4. SOME TYPICAL CAMBER LINES.

FIG. 5.

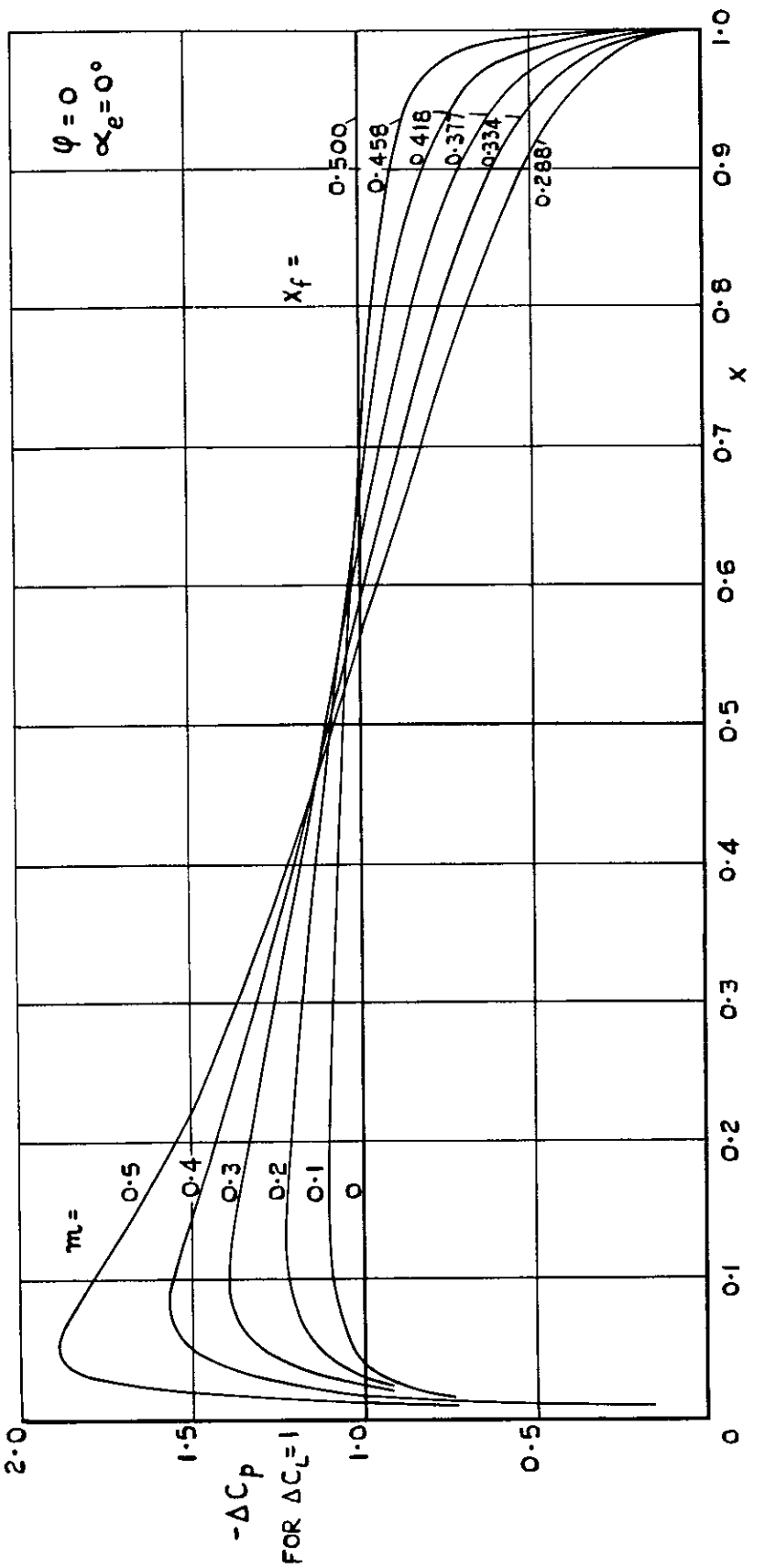

FIG. 5. SOME TYPICAL CHORDWISE LOADINGS.
(TWO-DIMENSIONAL WING)

FIG .6.

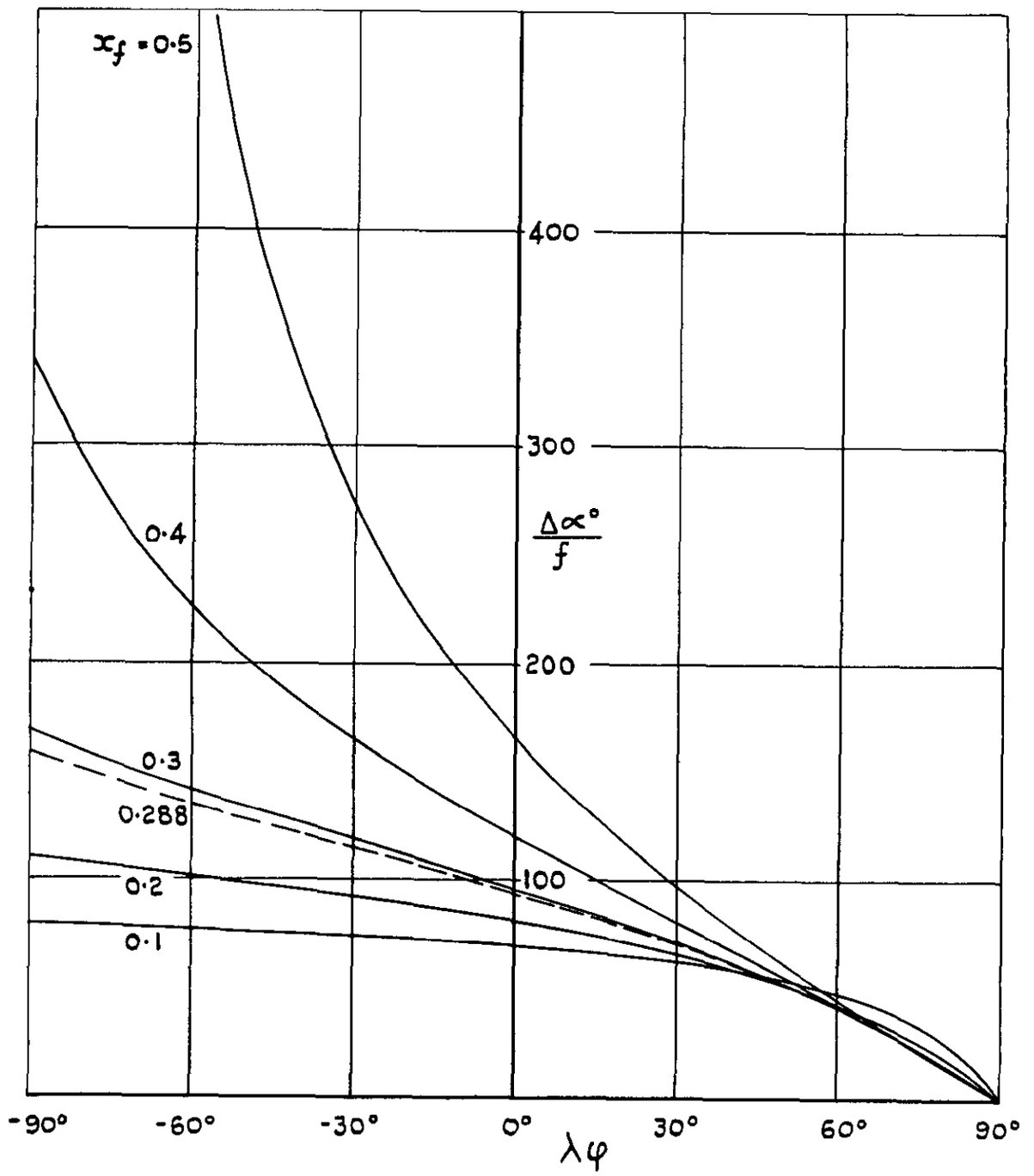

FIG.6. EQUIVALENT CHANGE OF INCIDENCE DUE TO CAMBER : $-90^\circ \leq \lambda\varphi \leq 90^\circ$.

FIG .7.

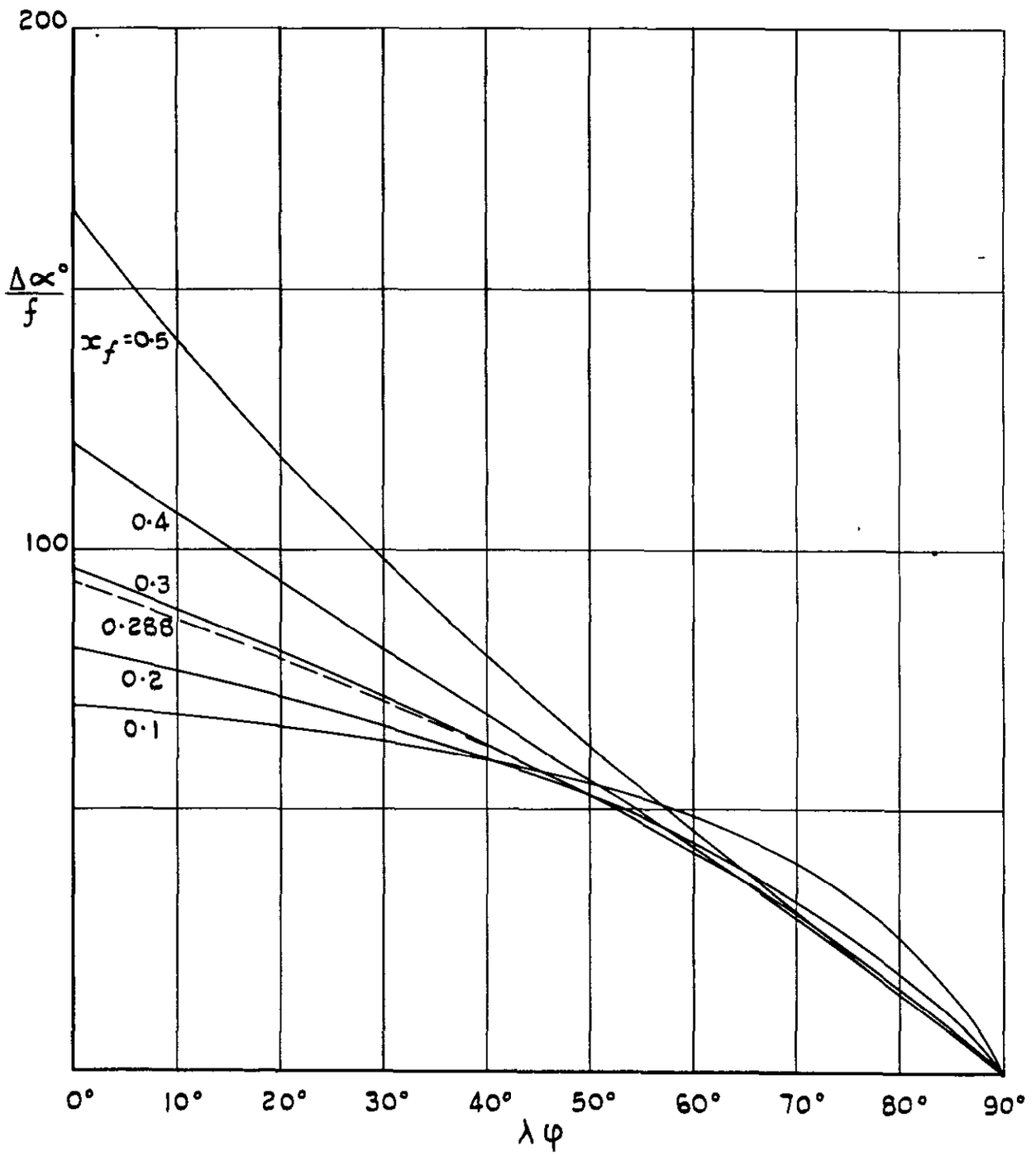

FIG. 7. EQUIVALENT CHANGE OF INCIDENCE DUE TO CAMBER : $0 \leq \lambda\varphi \leq 90^\circ$.

FIG. 8.

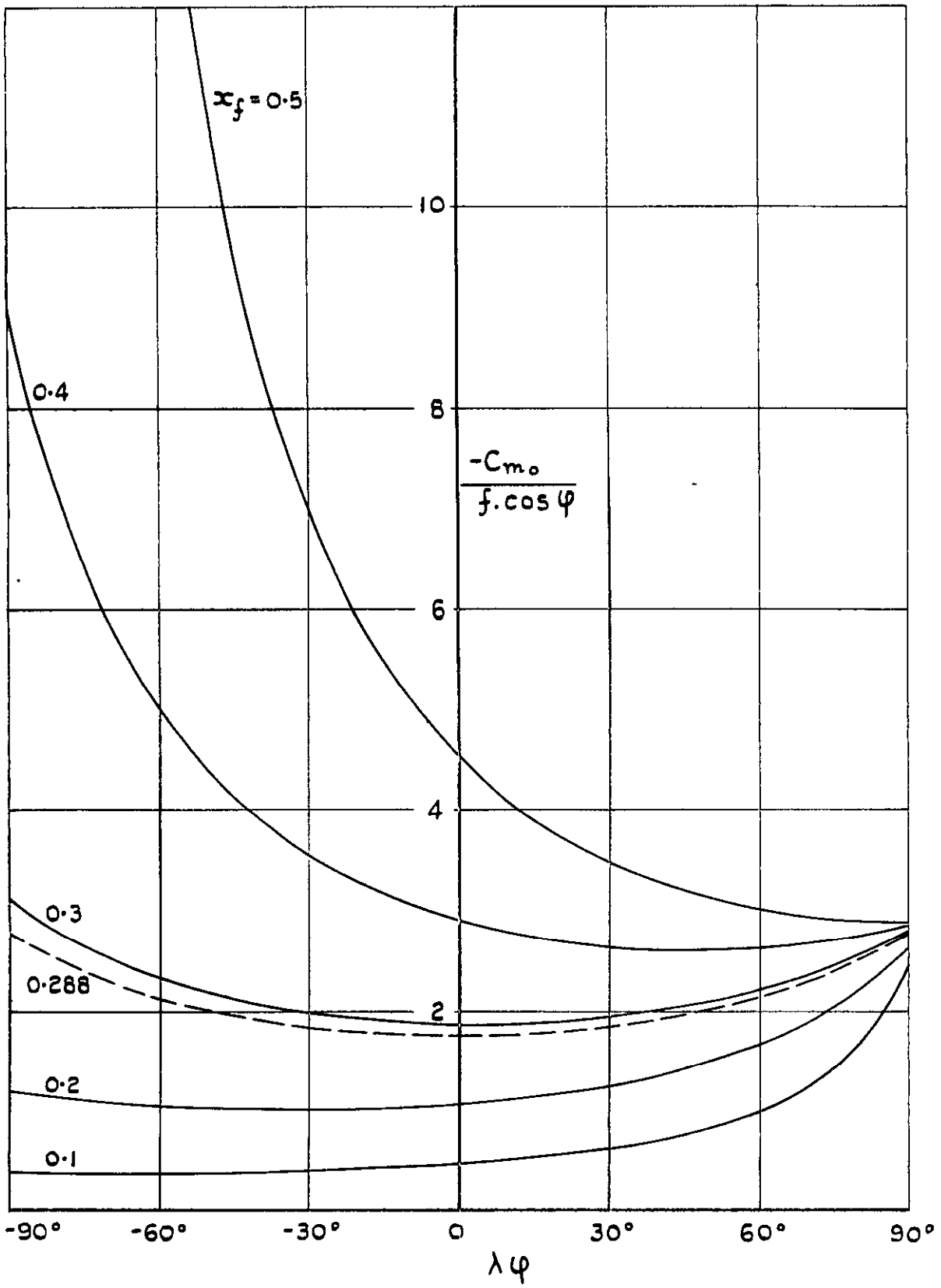

FIG. 8. PITCHING MOMENT AT ZERO LIFT.

FIG. 9 & 10.

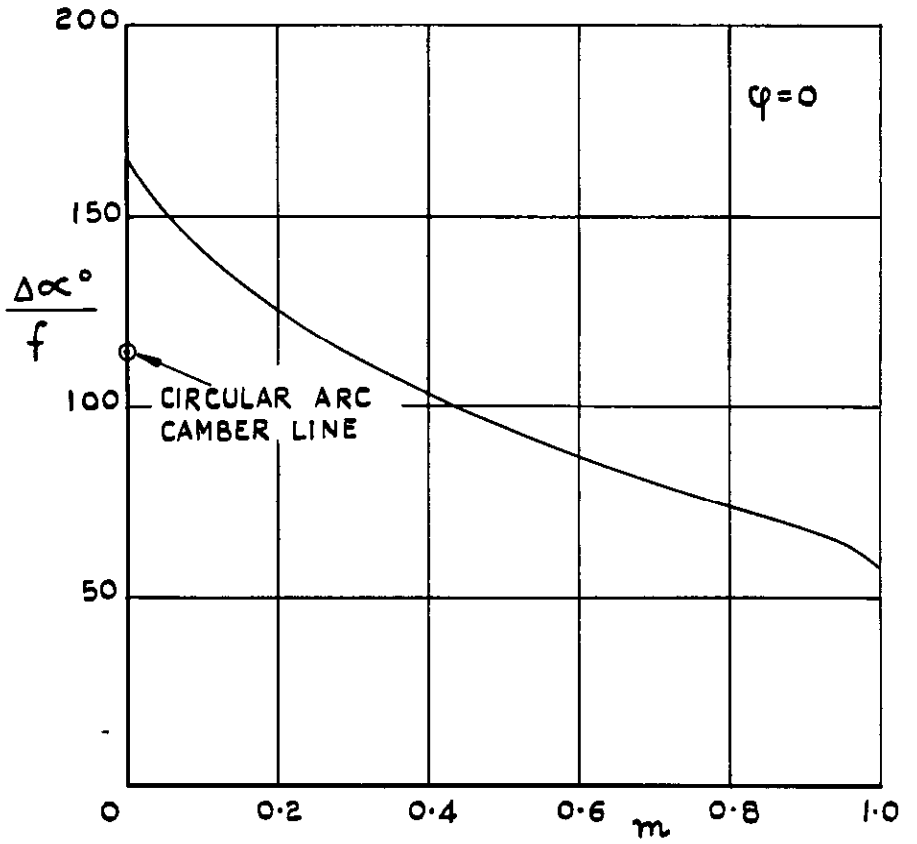

FIG. 9. EQUIVALENT CHANGE OF INCIDENCE DUE TO CAMBER (TWO-DIMENSIONAL WING).

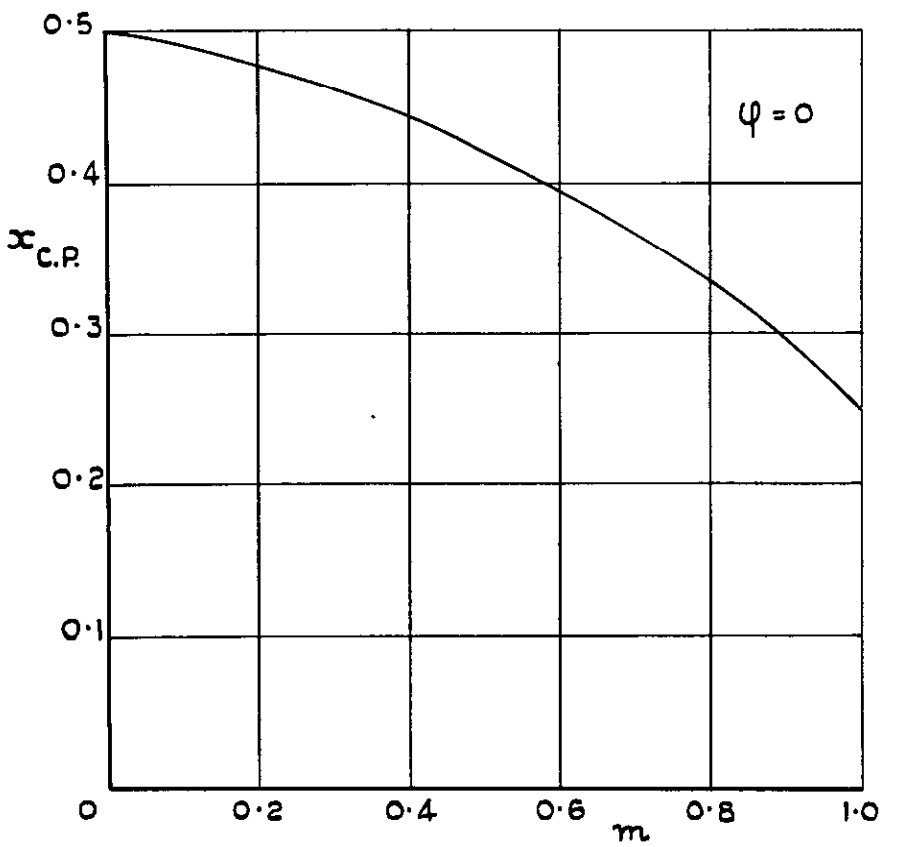

FIG. 10. CENTRE OF PRESSURE POSITION. (TWO-DIMENSIONAL WING).

FIG.11.

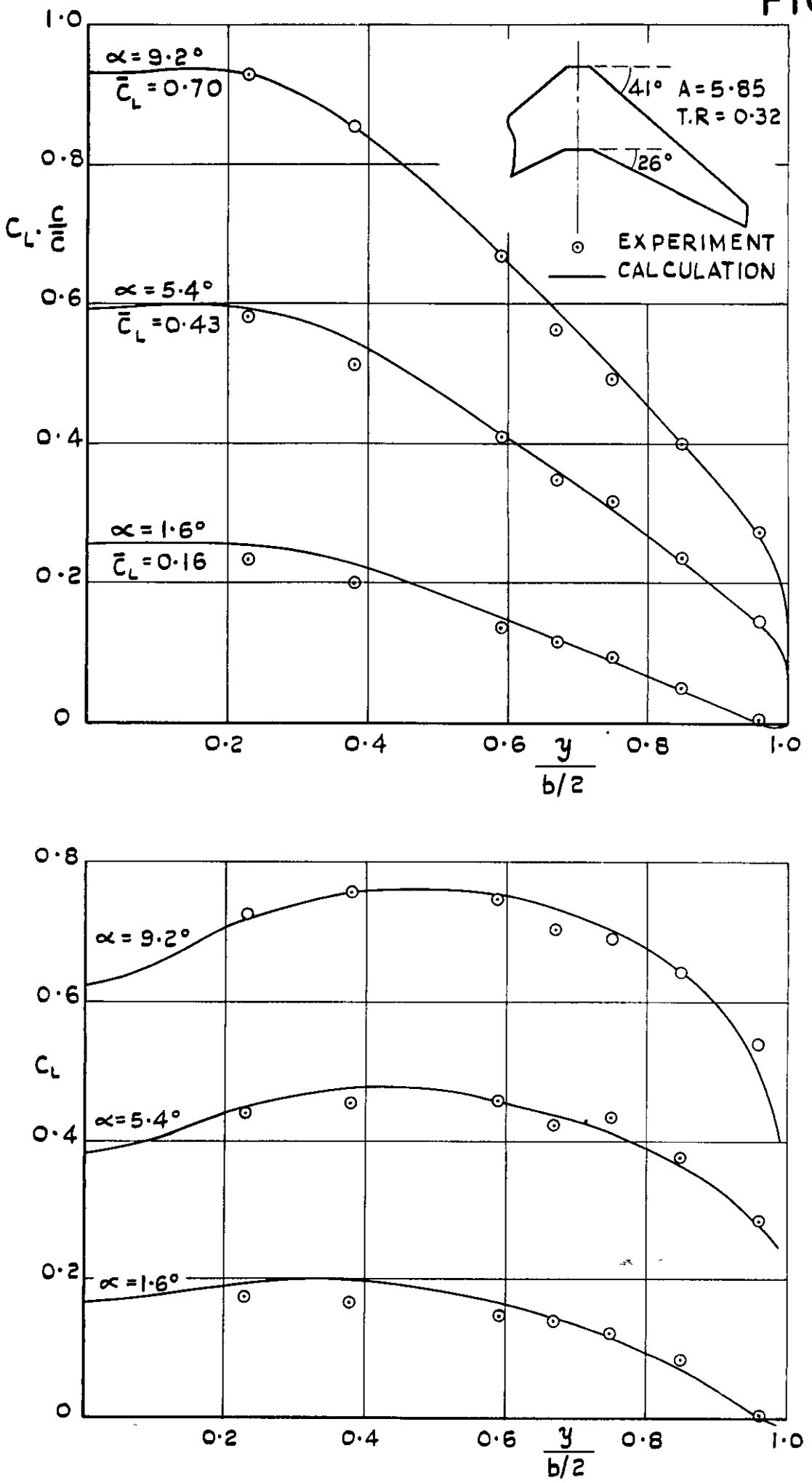

FIG.11. SPANWISE LOADING OF A WING WITH CAMBER AND TWIST (REF. 8).

FIG .12 & 13.

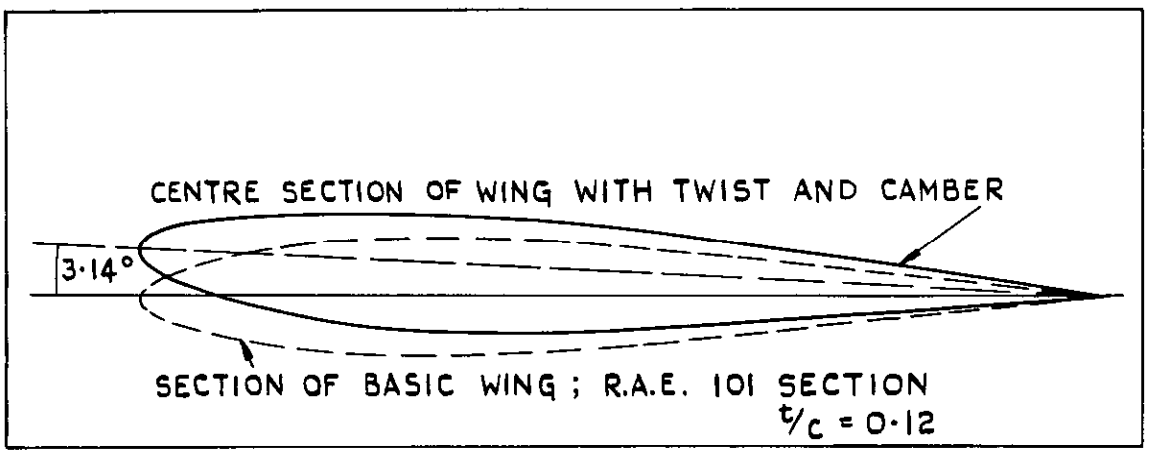

FIG.12. AEROFOIL SECTIONS ON WING WITH CAMBER AND TWIST (WING C, REF.4).

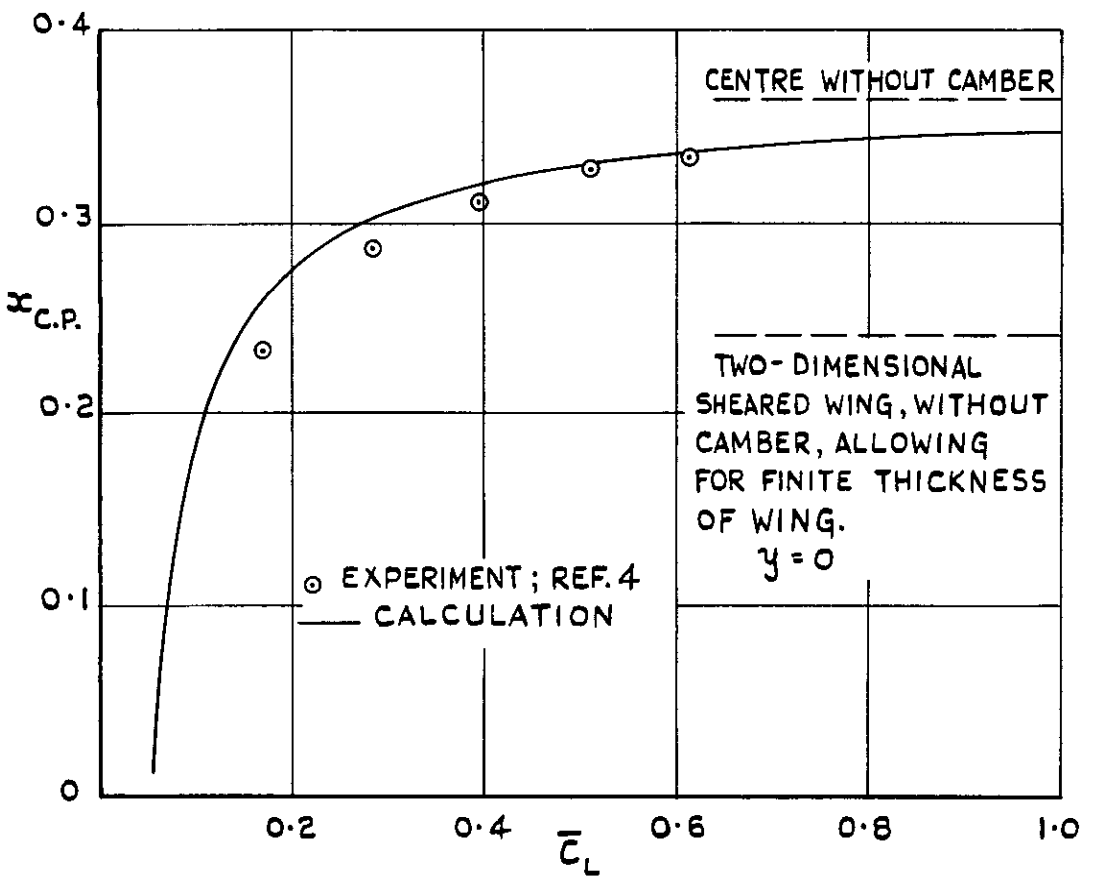

FIG.13. CENTRE OF PRESSURE POSITION AT CENTRE SECTION, (WING C, REF. 4).

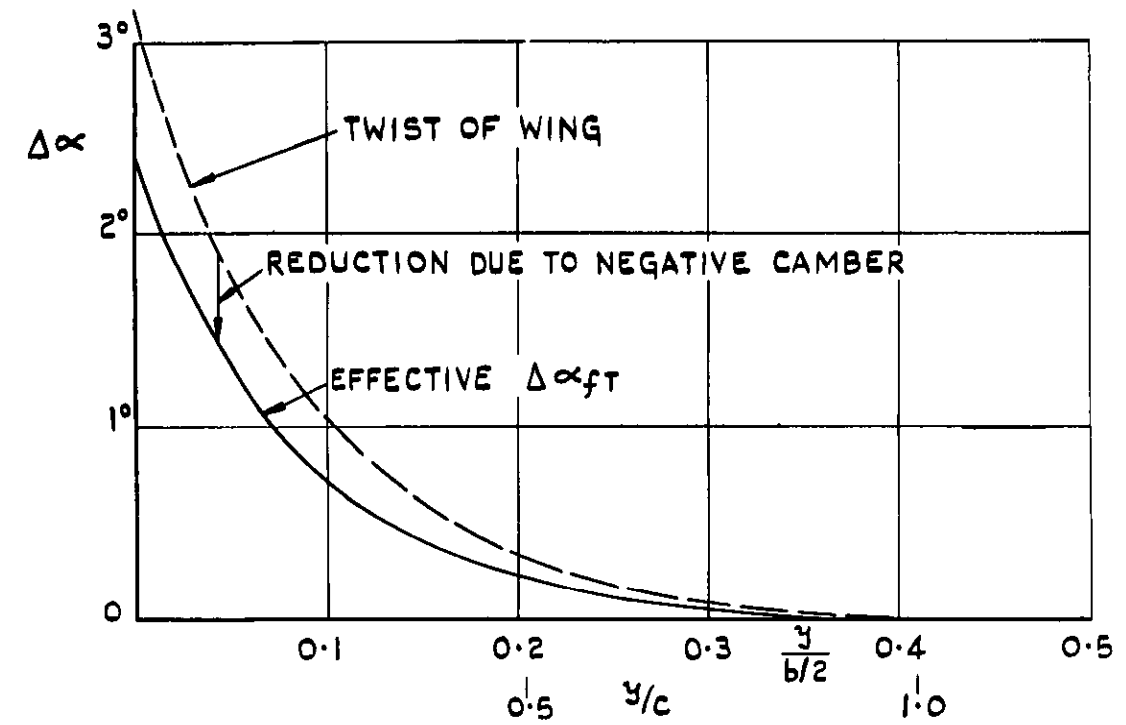

FIG.14. SPANWISE VARIATION OF TWIST (WING C, REF.4).

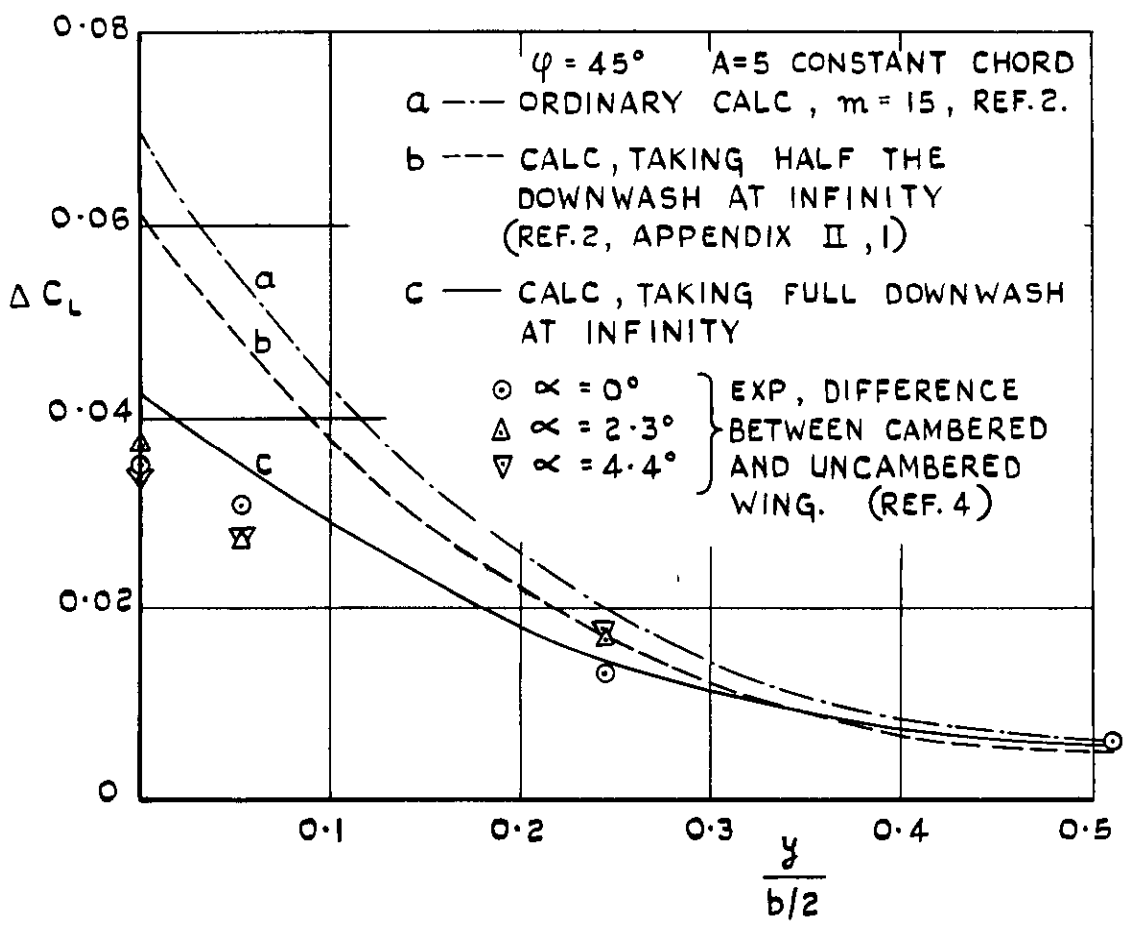

FIG.15. SPANWISE LOADING DUE TO TWIST AND CAMBER (WING C, REF.4).

FIG.16.

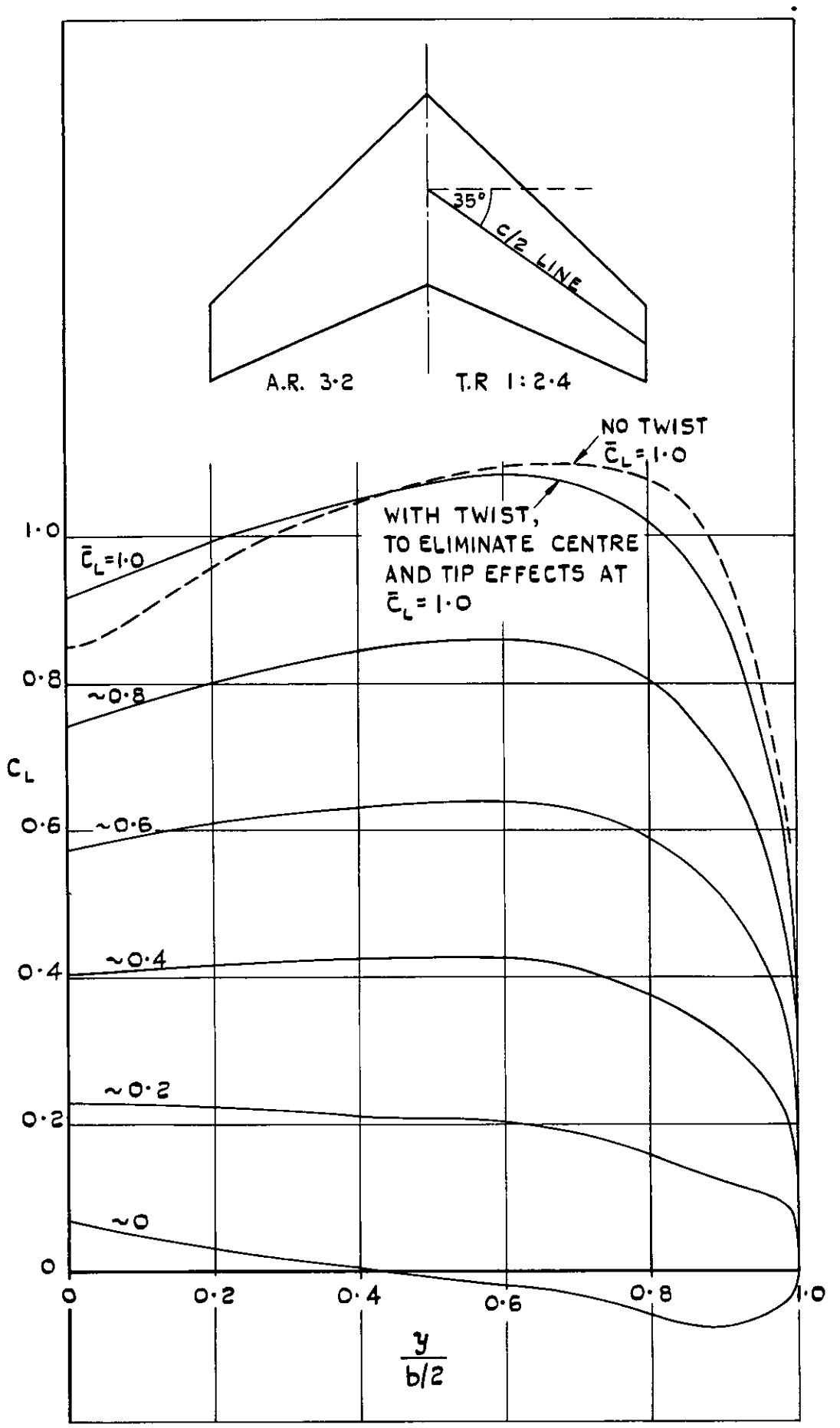

FIG.16. SPANWISE LOADING OF TWISTED WING, A.R. = 3·2.

FIG.17.

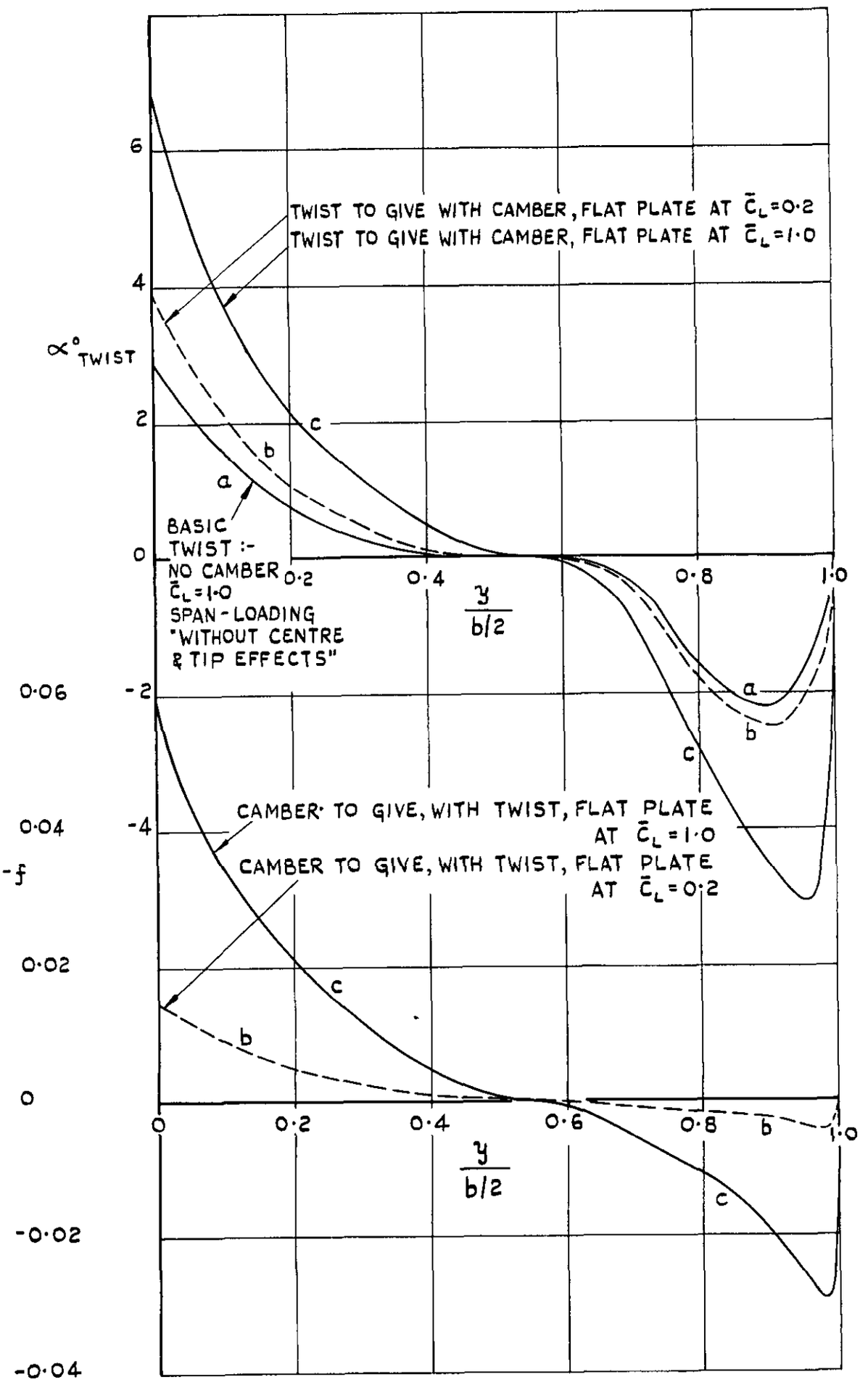

FIG.17. CAMBER AND TWIST TO GIVE VARIOUS LOADINGS ON A.R. 3·2 WING.

FIG.18 &19.

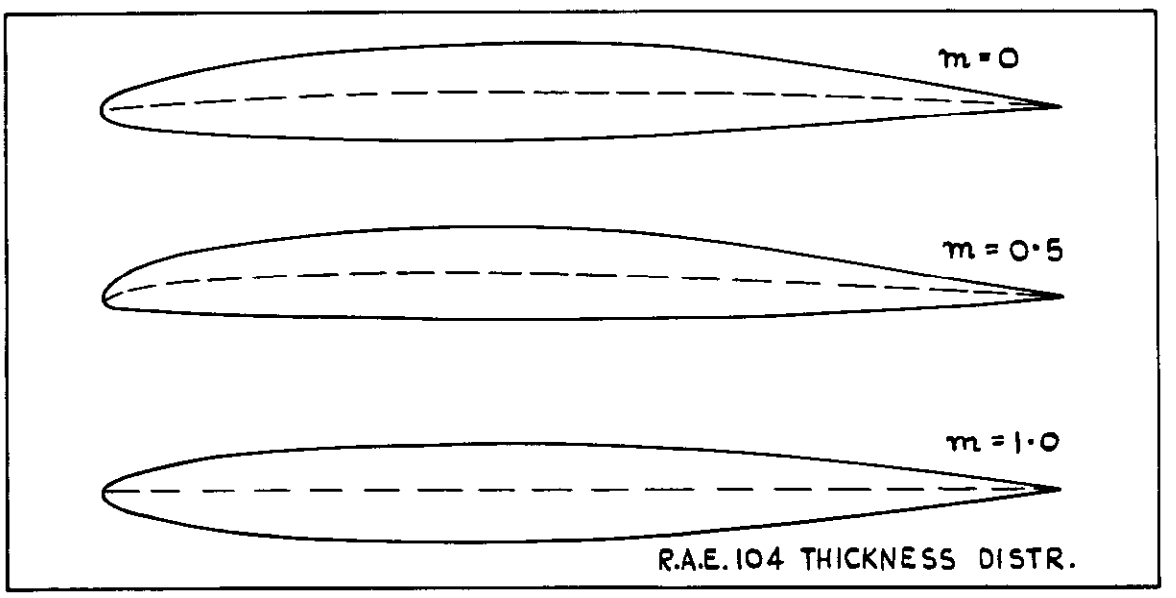

FIG.18. SOME TYPICAL THICK PROFILES.
t/c = 0·1.

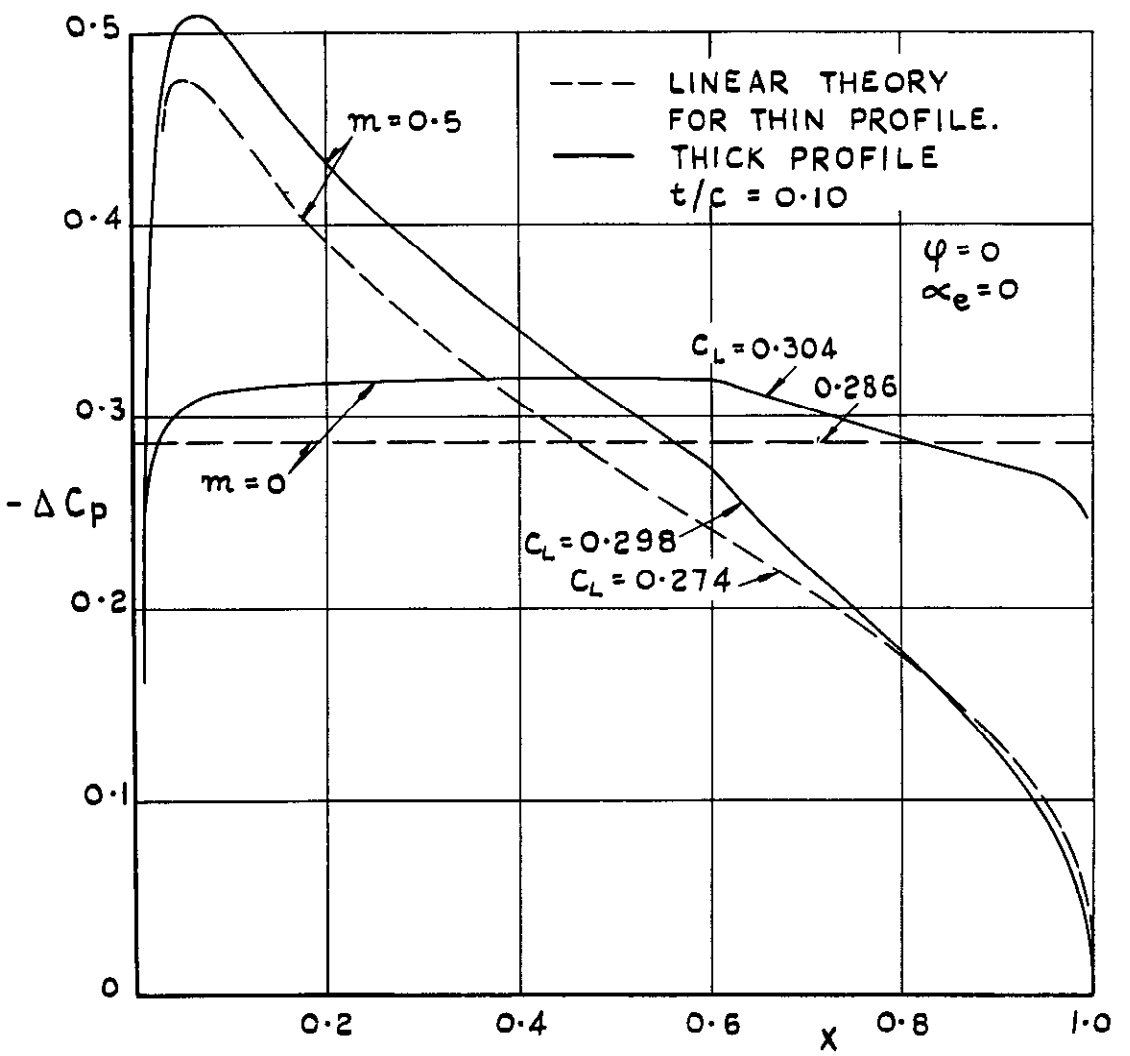

FIG.19. CALCULATED CHORDWISE LOADINGS ON TWO-DIMENSIONAL CAMBERED WINGS.

FIG.20.

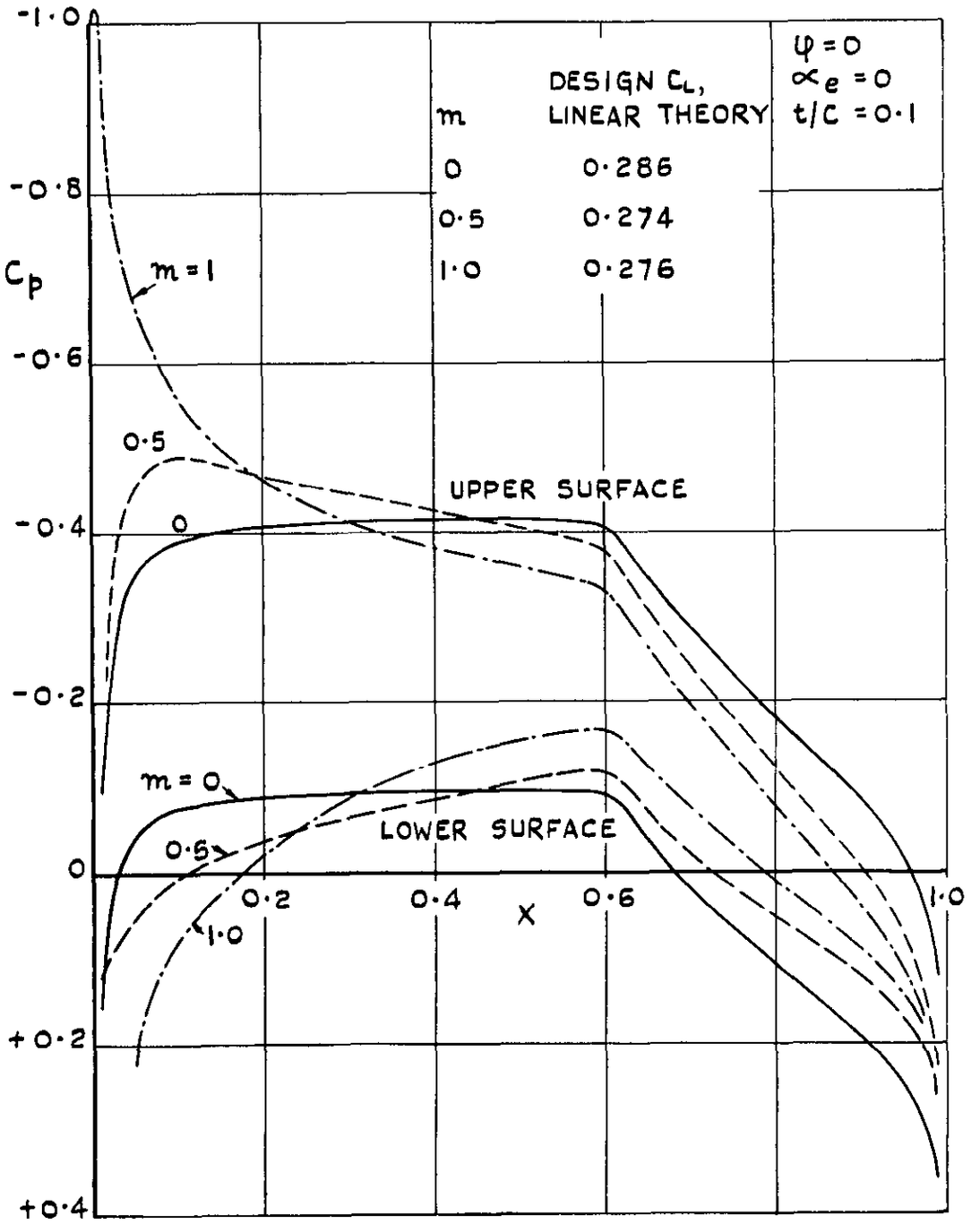

FIG.20. CALCULATED CHORDWISE PRESSURE DISTRIBUTIONS ON TWO-DIMENSIONAL CAMBERED AEROFOILS, $C_L \approx 0·3$. (R.A.E. 104 THICKNESS DISTRIBUTION).

C.P. No. 171
(15,177)
A.R.C. Technical Report

PUBLISHED BY HER MAJESTY'S STATIONERY OFFICE

To be purchased from

York House, Kingsway, LONDON, W C 2. 423 Oxford Street, LONDON, W 1
P.O. Box 569, LONDON, S E 1
13a Castle Street, EDINBURGH, 2 | 1 St Andrew's Crescent, CARDIFF
39 King Street, MANCHESTER, 2 | Tower Lane, BRISTOL, 1
2 Edmund Street, BIRMINGHAM, 3 | 80 Chichester Street, BELFAST
or from any Bookseller

1954

Price 5s. 6d. net

PRINTED IN GREAT BRITAIN

S.O. Code No. 23-9007-71